Effects of miR-141-containing extracellular vesicles in the regulation of endothelial tube formation by trophoblastic cells

Dissertation
zur Erlangung des akademischen Grades

doctor medicinae
(Dr. med.)

vorgelegt dem Rat der Medizinischen Fakultät
der Friedrich-Schiller-Universität Jena

von **Ruby Nicole Gutiérrez-Samudio**
geboren am **12. 12. 1987** in **Chiriquí, Republic of Panama**

Gutachter

1.

2.

3.

Tag der öffentlichen Verteidigung: ....

A mi querida familia, por su infinito

apoyo y preocupación.

To my dear family, for their infinite

support and concern.

TABLE OF CONTENTS

LIST OF ABBREVIATIONS

ATCC: American Type Culture Collection

BP: blood pressure

CT: cytotrophoblast

CTR: control

DMSO: Dimethyl sulfoxide

ECGM: Endothelial Cell Growth Medium

EHS: Engelbreth-Holm-Swarm (mouse sarcoma)

EMT: epithelial-mesenchymal transition

EVs: extracellular vesicles

EVT: extravillous trophoblasts

EXO: exosomes

FBS: Fetal Bovine Serum

GFR: Growth Factor Reduced

H: hours

HUVEC: Human Umbilical Vein Endothelial Cells

ILV: intraluminal vesicles

miRNAs: microRNAs

ml: milliliters

min: minutes

MMP: matrix metalloproteinases

MV: microvesicles

MVB: multivesicular bodies

NTA: nanoparticle tracking analysis

PBS: phosphate-buffered saline

pri-miRNAs: primary miRNAs

pre-miRNA: precursor miRNA

RT: room temperature

SCR-mimic: scramble mimic

SEM: standard error of the mean

ST: syncytiotrophoblast

TBS: Tris-Buffer Saline

TBS-T: Tween20 in TBS

SUMMARY

Preeclampsia constitutes a hypertensive disorder exclusive to pregnancy. It is a systemic disease with multi-organ involvement that complicates between 2 - 8% of all pregnancies, remaining one of the primary causes of maternal and perinatal morbidity and mortality in the world. Preeclampsia has been associated with improper extravillous trophoblast invasion into uterine spiral arteries and deficiency of their remodeling. Previous studies have revealed that trophoblast cells secrete microRNAs (miRNAs) into the maternal circulation by packing them within extracellular vesicles (EVs). This process takes place in normal and in preeclamptic pregnancies, but at different quantities and qualities, indicating its potential role in physiology and pathology of the placenta. EVs are present in maternal plasma from early pregnancy onwards, which represents potential diagnostic tools as biomarkers for gestational pathologies.

Previous studies in our lab showed that miR-141 expression is higher in placentas from preeclamptic compared to normal pregnancies. miR-141 is a pregnancy-related miRNA known to control trophoblast functions and to be associated with the process of angiogenesis. The aim of this study was to further investigate the role of miR-141 in the vascular remodeling of endothelial cells by trophoblastic cells using a 3D *in vitro* co-culture model of Human Umbilical Vein Endothelial Cells (HUVEC) and trophoblastic cells (HTR8/SVneo and JEG-3 cells).

The 3D co-culture model was established for quantitative evaluation of vascular tube-like formations as a method. When HTR8/SVneo cells were co-cultured with HUVEC, the tube formations were more permanent and stable, simulating the interaction between endothelial and trophoblast cells, and thus the remodeling of uterine spiral arteries in pregnancy.

Trophoblastic cells were modified by transient transfection to mimic miR-141 levels as observed in preeclampsia. Overexpression of miR-141 in HTR8/SVneo cells resulted in a highly significant disruption of tube formations when co-cultured with HUVEC, but this effect was not evident when using JEG-3 cells. Due to the poor

interaction between HUVEC and JEG-3 cells, only HTR8/SVneo cells were used to investigate the effect of miR-141-containing EVs on the tube formation.

Supernatant from miR-141-mimic transfected HTR8/SVneo cells was used to obtain EV-enriched fractions through differential ultracentrifugation. Subsequent characterization of EVs was done by using a Nanoparticle Tracking Analysis (size and concentration) and membrane proteins were confirmed with a Dot-Blot technique. Characterized EVs from transfected and control cells were added to non-modified HTR8/SVneo cells in the 3D cell culture model. Changes in the tube formation were evaluated through microscopy and image analysis. This treatment showed a similar disruptive effect, result appreciated with the co-culture of transfected trophoblastic cells and HUVEC.

Consequently, we can conclude that miR-141 is involved in the regulation of the angiogenic potential of trophoblastic cells. This regulation may be affected by communication between endothelial cells and miR-141-containing trophoblast-derived EVs. These effects may be related to processes during uterine spiral arteries remodeling and its disorders, such as the development of preeclampsia.

ZUSAMMENFASSUNG

Die Präeklampsie stellt eine hypertensive Störung ausschließlich während der Schwangerschaft dar. Es handelt sich um eine systemische Erkrankung mehrerer Organe, die bei 2 - 8% aller Schwangerschaften auftritt. Sie ist somit eine der Hauptursachen für mütterliche und perinatale Morbidität und Mortalität in der Welt. Präeklampsie wurde mit einer gestörten extravillösen Trophoblastzellinvasion in den Uterusspiralarterien und einem Mangel in ihrem Umbau in Verbindung gebracht. Frühere Studien haben gezeigt, dass Trophoblastzellen extrazelluläre Vesikel (EVs) in den mütterlichen Kreislauf sezernieren, welche microRNAs (miRNAs) enthalten. Dieser Prozess findet in normalen und in präeklamptischen Schwangerschaften statt, jedoch variieren sowohl Vesikelmenge als auch deren Inhalt, was auf eine potentielle Rolle der EVs in der Physiologie und Pathologie der Plazenta hindeutet. Trophoblastäre EVs sind ab der frühen Schwangerschaft im mütterlichen Plasma vorhanden und haben daher das Potenzial als Biomarker für die Diagnose von Schwangerschaftspathologien.

Frühere Studien in unserem Labor zeigten, dass die Expression von miR-141 in der Plazenta von präeklamptischen Schwangerschaften im Vergleich zu normalen Schwangerschaften höher ist. miR-141 ist eine schwangerschaftsassoziierte miRNA, der die Kontrolle von Trophoblastzellfunktionen zugeordnet wird, und die in die Regulation der Angiogenese involviert ist. Das Ziel dieser Studie war es, die Rolle von miR-141 beim vaskulären Umbau von Endothelzellen durch trophoblastären Zellen zu untersuchen. Dafür wurde ein 3D-*in-vitro* Co-Kulturmodell von *Human Umbilical Vein Endothelial Cells* (HUVEC) und trophoblastären Zellen (HTR8/SVneo- und JEG-3-Zellen) verwendet.

Die 3D-*in-vitro* Zellkultur wurde als eine Methode etabliert, welche die extrazelluläre Matrix simuliert und die quantitative Analyse von Veränderungen an der räumlichen kapillaren Wachstumsstruktur der Zellen (Tubusbildung) ermöglicht. HTR8/SVneo-Zellen, die in Matrigel ausgesät werden, wachsen in einem tubulären Netzwerk wobei sie einen endothelialen Phänotyp annehmen. Bei gleichzeitiger Kultivierung mit HUVEC leitet diese Eigenschaft auch die HUVEC zu einer verstärkten

Ausbildung von Tubusstrukturen und simuliert die Bildung der uterinen Spiralarterien während der Schwangerschaft.

Die trophoblastären Zellen wurden durch transiente Transfektion mit miR-141 modifiziert, um miR-141-Spiegel wie bei der Präeklampsie zu imitieren. Die Überexpression von miR-141 in HTR8/SVneo-Zellen führte bei deren Co-Kultur mit HUVEC zu einer hochsignifikanten Unterbrechung dieser Tubusbildung. Dieser Effekt war jedoch bei Verwendung von JEG-3-Zellen nicht erkennbar. Aufgrund der geringen Wechselwirkung zwischen HUVEC und JEG-3-Zellen wurden nur HTR8/SVneo-Zellen verwendet, um die Wirkung von EVs mit modifiziertem miR-141-Gehalt auf die Tubusbildung zu untersuchen.

Der Zellkultur-Überstand von miR-141-transfizierten Zellen wurde verwendet, um die EV-angereicherte Fraktionen durch differentielle Ultrazentrifugation zu erhalten. Die anschließende Charakterisierung erfolgte unter Verwendung der Nanopartikel-Tracking-Analyse (Bestimmung der Größe und Konzentration der EVs) und der Nachweis von Membranproteinen erfolgte über eine Dot-Blot-Technik. Die unterschiedlichen EVs wurden dann zur 3D-Co-Kultur nicht-modifizierter HTR8/SVneo-Zellen mit HUVEC hinzugefügt. Änderungen in der Tubusbildung aufgrund der jeweiligen EV-Zugabe wurden durch Mikroskopie und Bildanalyse bestimmt. Die Zugabe von EVs mit erhöhten miR-141 Konzentrationen zu den Co-Kulturen von HTR8/SVneo-Zellen und HUVEC hatte ähnliche Wirkungen auf die Angiogenese wie die direkte miR-141-Transfektion der HTR8/SVneo-Zellen.

Daraus lässt sich schlussfolgern, dass miR-141 eine Beteiligung an der Regulation des angiogenen Potentials trophoblastärer Zellen hat. Es wird vermutet, dass diese Regulation durch die Kommunikation zwischen Trophoblastzellen und Endothelzellen durch miR-141-haltige EVs beeinflusst wird. Wir vermuten, dass die beobachteten Effekte Prozesse des gestörten vaskulären Umbaus der Uterusspiralarterien bei einer Präeklampsie widerspiegeln.

1. INTRODUCTION

During human pregnancy, the placenta allows the exchange of gasses and nutrients between the mother and the fetus. The maternal blood that surrounds the syncytiotrophoblasts in the intervillous space interacts with the fetal capillary blood within the connective tissue at the villous core (Wang and Zhao 2010). This interaction can be disrupted by an inappropriate remodeling of the uterine spiral arteries, causing disturbances during pregnancy, such as preeclampsia.

Preeclampsia is one of the clinical syndromes that remains the primary cause of maternal and perinatal morbidity and mortality in the world (Powe, Levine et al. 2011). It also occurs in molar pregnancies, indicating that it relays more on the placenta than in a fetal origin (Ahmed and Ramma 2015). Thus far, the only curative treatment for preeclampsia is termination of pregnancy. Therefore, the possibility to find a premature detection of this disease through biomarkers has been studied in the last years.

Biomarkers are molecules that objectively identify, in a quantitative way, a normal or a pathological situation (Strimbu and Tavel 2010). In pregnancy, fetal miRNAs can be found in the maternal circulation from early pregnancy onward, via EVs, but at different quantities and qualities (Burton and Jauniaux 2015). These differences in content and the fact that EVs are found in maternal blood is what makes these particles essential for early detection of preeclampsia.

1.1. Implantation, Invasion, and Placentation

1.1.1. **Implantation**

After fertilization, the conceptus follows a series of steps leading to its implantation into the maternal endometrium (Imakawa, Bai et al. 2017):

- *Transport of the conceptus*

  During the next days after fertilization, the zygote, a diploid cell with 46 chromosomes is transported from the ampulla of the fallopian tube into the uterine cavity. The zygote suffers a continuous process of cell proliferation, without volume increase, until it becomes a solid collection of multiple cells surrounded by the *zona pellucida*, called morula.

- *Blastocyst formation*

  Around the 4th – 6th day after fertilization, gradual accumulation of fluid between the cells of the morula results in the formation of the early blastocyst (Cunningham and Williams 2010). The inner cell mass of the blastocyst (embryoblast) will develop as the actual embryo, and the outer flat cells will compact to each other to form the trophoblast.

- *Embryo implantation*

  In humans, the window of implantation occurs 6 – 10 days after ovulation (Su and Fazleabas 2015). It starts with an adhesion phase, where the embryoblast already emerged from the *zona pellucida* and adheres itself into the uterine epithelium, facing the endometrium, commonly in the superior and posterior walls of the uterine body. When the embryoblast does not face the endometrium, it migrates along the inside face of the trophoblast to align itself. The firm adhesion of the blastocyst is recognized as the attachment phase, and it cannot be removed, starting the process of invasion.

1.1.2. **Trophoblast invasion and placentation**

The trophoblasts migrate into the endothelium and fuse to become the syncytiotrophoblast (ST). Meanwhile, the rest of the trophoblasts, now called cytotrophoblast (CT), surround the embryoblast and form columns. These structures break through the ST layer to form the primary chorionic villi and give rise to villous and extravillous trophoblasts (EVT). This process is considered as the beginning of placentation. The villous trophoblasts are responsible for the exchange of oxygen and nutrients between fetus and mother. By the 10th week of pregnancy, the EVT colonize the opening wall of the maternal uterine spiral arteries because of their high invasion ability (Cunningham and Williams 2010).

1.1.3. **Uterine spiral arteries remodeling**

- *Physiological changes*

   The EVT are further classified as interstitial and endovascular trophoblasts. The interstitial trophoblasts migrate through the endometrial stroma, penetrate the walls of the uterine spiral arteries from outside, and present characteristics of an epithelial to mesenchymal transition (EMT) (Soares, Chakraborty et al. 2014). During EMT, important step in the invasion, the epithelial cells lose their apicobasal polarity and the tight cell-cell adhesion resulting in a mesenchymal phenotype and improved migratory abilities, by downregulation of E-cadherin and upregulation of Vimentin and N-cadherin (Senfter, Madlener et al. 2016).

   Meanwhile, the endovascular trophoblasts migrate to the lumen, modify the smooth muscle layer of the uterine spiral arteries by a partial replacement of the endothelial cells, and display an epithelial to endothelial-like transformation (Soares, Chakraborty et al. 2014). By accumulation, the endovascular trophoblasts cause an occlusion known as the spiral arteriole plug, which reduces the maternal blood flow leaving the embryo nourishment depending on the endometrial glands (Degner, Magness et al. 2017).

   The uterine spiral arteries suffer different changes on the cellular and extracellular constituents including migration, hyperplasia, apoptosis, and extracellular matrix remodeling. Because of the replacement of the tunica media, the spiral arteries lose their compression ability, changing from narrow

into wide conduits, with reduced resistance to blood flow. In order to keep up with the growing metabolic needs of the fetus, the spiral arteries often reach 500 µm in diameter at the end of pregnancy (Degner, Magness et al. 2017). The blood flow increases from about 45 ml/min in the non-pregnant uterus to approximately 750 ml/min at term (Burton, Woods et al. 2009).

- *Pathological changes: improper EVT invasion*

  Defective EVT invasion into the uterine spiral arteries and the resulting deficiency of their remodeling have been associated with preeclampsia, (O'Tierney-Ginn and Lash 2014). The uterine spiral arteries in preeclampsia remain with a mean diameter of 200 µm, similar to the size and composition as seen in non-pregnant women (the comparison is shown in Figure 1). Also, in preeclampsia, these vessels are still responsive to vasomotor stimuli, causing a decrease in the uteroplacental perfusion pressure and restricting the blood supply to the fetus (Degner, Magness et al. 2017). These alterations can lead to placental ischemia/hypoxia and alteration in the maternal immune response, leading to systemic endothelial dysfunction which appears as the common clinical features seen in preeclampsia.

The detection of disturbances in the placental flow is possible after the 12th week of gestation, period of time when the maternal blood flow toward the placenta is established (Huppertz 2008). Although disturbances are noticed by ultrasonography, it is worth saying that it is not a unique characteristic of preeclampsia and not enough for a proper diagnosis. The establishment of a proper and early diagnosis will improve the antenatal and perinatal care.
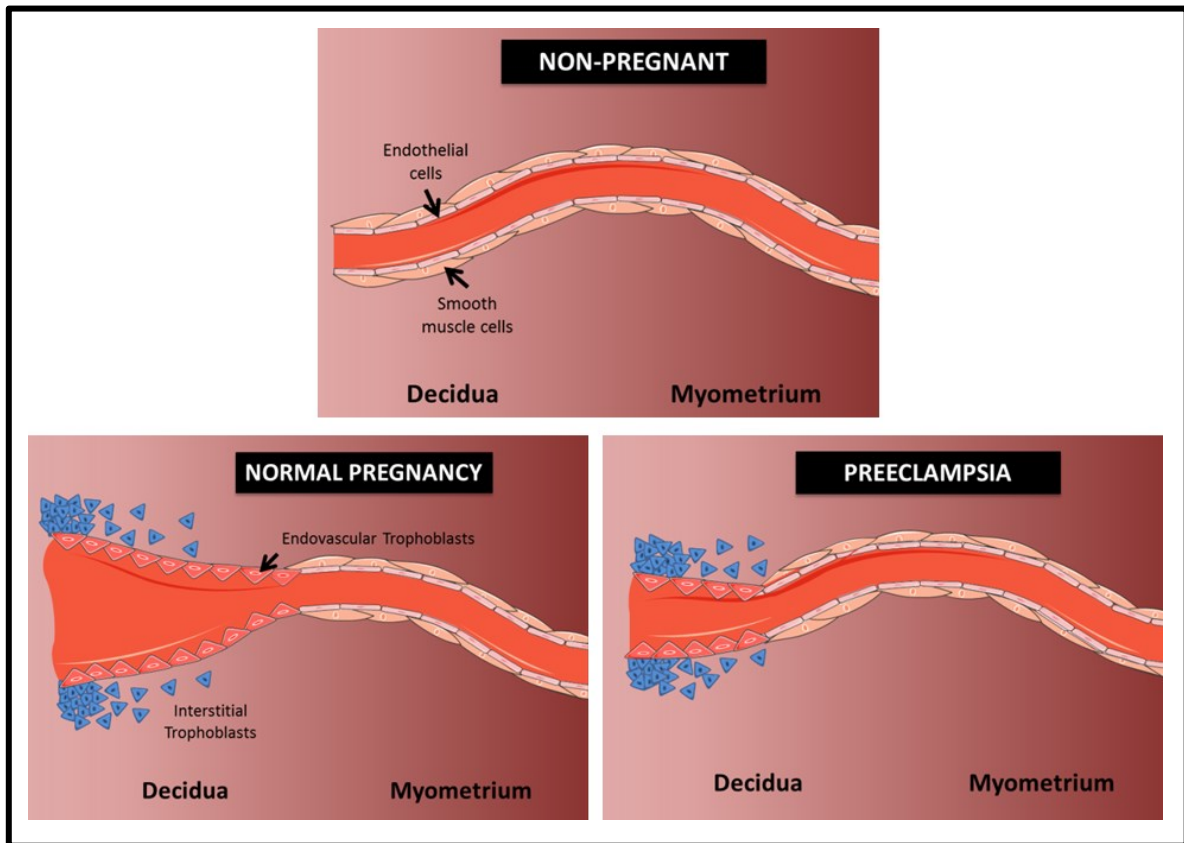
Figure 1. Uterine spiral arteries during physiological or pathological processes. During normal pregnancy, uterine spiral arteries widen and often reaching 500 μm in diameter at the end of pregnancy. This effect is not seen in preeclampsia because of the poor EVT invasion, remaining with a mean diameter of 200 μm, similar size, and composition of the ones seen in non-pregnant women.

1.2. Preeclampsia

1.2.1. **Epidemiology**

Preeclampsia is a multisystem hypertensive disorder and one of the primary causes of maternal and perinatal morbidity and mortality in the world. It affects between 2 - 8% of all pregnancies and is responsible for 9 – 26% of the maternal deaths worldwide (Townsend, O'Brien et al. 2016). Its onset is multifactorial: more common in African-American women, low socioeconomic status, multifetal gestation and *primigravidas* (Steegers, von Dadelszen et al. 2010). Preeclampsia is increasing nowadays due to higher maternal age, obesity, and other medical comorbidities, as diabetes and hypertension; and a need for early detection and treatment is required to improve maternal and neonatal health (WHO 2011).

1.2.2. **Clinical features**

The International Society for the Study of Hypertension in Pregnancy (ISSHP) has re-defined preeclampsia as *de-novo* hypertension after 20 weeks of gestation: blood pressure (BP) ≥ 140 mmHg systolic or ≥ 90 mmHg diastolic, on 2 occasions at least 6 h apart, while the patient is on bed rest; combined with the onset of one or more of the following conditions (Bokslag, van Weissenbruch et al. 2016):

    a. Proteinuria, or

    b. Maternal organ dysfunction

- renal insufficiency
- liver involvement
- neurological complications
- hematological complications

    c. Uteroplacental dysfunction (fetal growth restriction)

1.2.3. **Classifications**

- *Clinical: mild vs severe*

  The disease severity is based on the BP measurement and whether there are signs of systemic involvement (Tranquilli, Dekker et al. 2014).

  o Mild / moderate: BP 140 - 159 mmHg systolic and/or 90 - 109 mmHg diastolic, plus:

    ▪ Proteinuria ≥ 300 mg/day or ≥ 2+ on dipstick testing (on 2 random urine samples, collected at least 4 h apart)

    ▪ In the absence of proteinuria, any of the following:

      ✓ Serum creatinine ≥ 1.02 mg/l

      ✓ Elevated blood concentrations of liver transaminases to twice normal concentration; epigastric abdominal pain

      ✓ Cerebral or visual disturbances: altered mental status, hyperreflexia, severe headaches with or without visual scotomas, tinnitus, phosphene signals

      ✓ Thrombocytopenia (platelets count < 150,000/dl)

  o Severe

    ▪ BP ≥ 160 mmHg systolic and/or ≥ 110 mmHg diastolic

    ▪ Proteinuria

    ▪ In the absence of proteinuria, any of the symptoms or signs mentioned in mild preeclampsia

- *Time of onset: early vs late* (Huppertz 2008)

  o Early

    ▪ Less than 34 weeks of pregnancy (34 + 0)

    ▪ Most severe and higher rates of maternal and neonatal morbidity and mortality (usually, fetal growth restriction)

    ▪ Inadequate trophoblast invasion of the uterine spiral arteries

  o Late

    ▪ More than 34 weeks of pregnancy (34 + 1)

    ▪ Normally grown neonate

    ▪ Mother frequently with previous (multiples) pregnancies or/and pathological complications (diabetes mellitus, anemia, obesity)

- *Etiology: placental vs maternal*

  The severity and progression of preeclampsia are significantly affected by the maternal response to placental derived factors and proteins. Therefore, preeclampsia can be divided by inducement of placental or maternal factors.

  - Placental factors. This concept is based on the failure to transform the maternal spiral arteries, caused by the inadequate EVT invasion. This leads the uterine spiral arteries to remain narrow and with high pressure affecting the normal development of the placenta: low maternal blood flow, hypoperfusion, ischemia, and hypoxia of the placenta (Li, Ge et al. 2013). The circulation in the intervillous spaces become abnormal, damaging the villous branches, filling it with thrombotic material, and later detected in the peripheral maternal blood, causing systemic endothelial alterations (Burton, Woods et al. 2009). These endothelial dysfunctions cause microangiopathic hemolytic anemia and vascular hyperpermeability associated with low serum albumin inducing edema, particularly in the lower limbs or lungs (Uzan, Carbonnel et al. 2011).

  - Maternal factors. This takes place in women with previous vascular dysfunction exacerbated by pregnancy, such as obesity, hypertension or diabetes (Craici, Wagner et al. 2014). The vascular stress leads to damages in the endothelium and contributes to the development of preeclampsia (Gilani, Weissgerber et al. 2016). The maternal etiology is sometimes related to the late onset or with mild preeclampsia; meanwhile, the placental etiology is related with the early onset or with severe preeclampsia (Steegers, von Dadelszen et al. 2010).

1.2.4. **Complications**

If preeclampsia is not detected on time and treated in order to maintain maternal hemostasia, pregnancy condition can worsen with severe complications (Townsend, O'Brien et al. 2016):

- *HELLP syndrome:* occurs in around 5% of mild preeclampsia or 10 – 20% of severe preeclampsia. It is described by **H**emolysis (and consequently, anemia), **E**levated **L**iver enzymes (presenting hepatic dysfunction), and **L**ow **P**latelets (less than 150,000/dl).

- *Eclampsia/cerebral hemorrhage*: eclampsia is defined as generalized tonic-clonic seizures that can lead to cerebral damage. Changes in the blood pressure can later cause hypertensive encephalopathy.
- *Renal impairment*: in normal pregnancy, renal perfusion and filtration increase and creatinine levels should be lower than normal. During preeclampsia, the glomerular endothelium is directly damaged, increasing the creatinine levels.
- *Pulmonary edema*: the low concentration of albumin in the blood leads to a reduction on the oncotic pressure and thus, a relative depletion of the intravascular volume with significant interstitial fluid, causing preeclamptic women to be vulnerable to pulmonary edema due to the significant renal impairment.
- *Other complications* (Mol, Roberts et al. 2016)
  - Rupture of the liver
  - Myocardial ischemia or infarction
  - Disseminated intravascular coagulation
  - Placenta-related complications, such as abruption

As long-term complications, affected women may suffer from stroke, cardiac ischemia, or venous thrombosis; and are vulnerable to a high risk of death from cardiovascular diseases (Gongora and Wenger 2015) (Powe, Levine et al. 2011). Children from mothers that suffered preeclampsia are at risk of preterm birth, fetal growth restriction or even fetal death (Bokslag, van Weissenbruch et al. 2016).

Many difficulties remain concerning prediction of preeclampsia. In this way, the study of this disease through biological markers present in blood is considered nowadays a closer possibility. Many diseases have been studied and related to miRNAs, molecules that can be detected in different body fluids during normal and pathological situations.

1.3. MicroRNAs

1.3.1. **Description**

miRNAs are short, single-stranded, non-coding RNAs (20 - 24 nucleotides), involved in post-transcriptional regulation of gene expression in multicellular organisms by affecting the stability and translation of mRNAs. miRNAs target sequences in the 3' untranslated regions (3'UTR) of the transcripts, mostly imperfectly, leading to mRNA degradation (Suarez and Sessa 2009). A single miRNA can bind and target multiple mRNAs and at the same time, one mRNA can be regulated by multiples miRNAs.

miRNAs are initially transcribed in the nucleus by the RNA polymerase II called primary miRNAs (pri-miRNAs) (Ha and Kim 2014); at the 5' end with a 5'-methyl-7-guanosine cap and at the 3' end, with a poly (A) tail (Gao, Feng et al. 2016). The nuclear microprocessor complex (composed by Drosha, a nuclear RNase III, and a double-stranded RNA binding protein), cleaves the pri-miRNA to release a hairpin-shaped precursor miRNA (pre-miRNA), which is transferred from the nucleus to the cytoplasm by the Exportin-5. When the pre-miRNA reaches the cytoplasm, it is processed by a complex containing Dicer, a specific RNase III endonuclease, and a double-stranded RNA-binding protein, liberating a miRNA duplex. The mature single-stranded form (guide strand) is incorporated into the RNA-induced silencing complex, repressing protein translation (Gregory and Shiekhattar 2005); while the complementary strand is released and typically degraded (Suarez and Sessa 2009). Circulating miRNAs are stable and protected from RNase degradation, which is achieved by their inclusion on either in various protein complexes or in different types of EVs (Cretoiu, Xu et al. 2016).

1.3.2. **miR-141**

Trophoblasts express different miRNAs that can be found in maternal blood, increasing throughout pregnancy and disappearing after delivery (Morales-Prieto, Chaiwangyen et al. 2012). The selection of the miR-141 for this project was based on previous studies in our lab demonstrating an importance in the regulation of trophoblast cells (Ospina-Prieto, Chaiwangyen et al. 2016). Furthermore, miR-141

is significantly higher expressed in plasma from pregnant compared to non-pregnant women, and it is overexpressed in preeclamptic compared to normal placentas.

miR-141 is a placenta-related miRNA, located in the gene 12p 13.31 (Li, Ge et al. 2013). It belongs to the miR-200 family which is composed of five miRNAs: miR-200a, -200b, -200c, -141, -429. The miR-200 family is organized into two genomic clusters but also into two functional groups. The clusters are located in chromosomes 1 (miR-200c / -200a / -429) and chromosome 12 (miR-200c and miR-141) (Senfter, Madlener et al. 2016). The functional groups, 1 and 2, differ by the third nucleotide of their sequence, either C or U, allowing some target genes to overlap (Pecot, Rupaimoole et al. 2013). The functional group 1 is composed by miR-141 and miR-200a, and the functional group 2, by miR-200b, -200c, and -429 (Figure 2). The miR-200 family has been shown to regulate different cellular processes, including inhibition of the EMT by downregulation of ZEB1 and ZEB2 (Gao, Feng et al. 2016). These genes are known to induce the expression of Matrix Metalloproteinases (MMP) that degrade the basement membrane, contributing to the trophoblast invasion (Imakawa, Bai et al. 2017).

				Seed																		
miR-141	U	A	A	C	A	C	U	G	U	C	U	G	G	U	A	A	A	G	A	U	G	G
miR-200a	U	A	A	C	A	C	U	G	U	C	U	G	G	U	A	A	C	G	A	U	G	U
miR-200b	U	A	A	U	A	C	U	G	C	C	U	G	G	U	A	A	U	G	A	U	G	A
miR-200c	U	A	A	U	A	C	U	G	C	C	G	G	G	U	A	A	U	G	A	U	G	G	A
miR-429	U	A	A	U	A	C	U	G	U	C	U	G	G	U	A	A	A	C	C	G	U	

■ Functional group 1

■ Functional group 2

Figure 2. Functional groups of the miR-200 family. Both functional groups share the same seeding sequence from position 2 to 7 from the miRNA 5'end, but groups' differences are found in the 3rd nucleotide.

1.4. Extracellular Vesicles

Since the 2000s, EVs have shown to play an important role in the horizontal transfer of coding and non-coding RNA, and other molecules, allowing the communication between several types of eukaryotic cells (Ratajczak, Miekus et al. 2006). This extends the idea that exosomes carry information that can be transferred from cell to cell either in normal conditions as well as in pathologies, such as preeclampsia.

1.4.1. **Description**

EVs are bilayer-membrane structures released from different cell types depending on their microenvironment. They are able to change the activity of contiguous or distant cells by traveling through blood circulation and releasing their content into the cytosol of target cells, and thus, involved in the cell-to-cell communication (Escudero, Herlitz et al. 2016) (Tannetta, Masliukaite et al. 2016). Aside from blood, EVs can also be isolated from different body fluids such as urine, cerebrospinal fluid, breast milk, semen, saliva and amniotic fluid.

The idea of micro-particles in blood exists since a few decades ago, when Peter Wolf in 1967, reported the presence of "platelet-dust" after a high-speed centrifugation (Wolf 1967). This fraction exerted coagulation properties, while the supernatant did not present the same qualities. In 1983, the term "exosomes" was first defined by Rose M. Johnstone while mapping the trafficking of the transferrin receptor in the maturation of reticulocytes (Johnstone, Adam et al. 1987). They found the release of small membrane vesicles that were previously formed in intracellular endosomes, which fused with the plasma membrane and later secreted to the exterior.

EVs are composed of different types of proteins, lipids and nucleic acids, such as mRNA and miRNA (Table 1). This content, protected from proteases and nucleases in the extracellular space, may vary depending on the biogenesis, cell type and surrounding conditions (Abels and Breakefield 2016).

Table 1. Frequent cargo of EVs, sub-classified in proteins, lipids, and nucleic acids
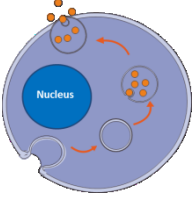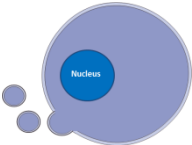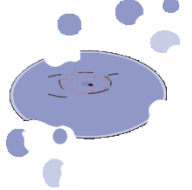
Proteins	○ CD63, CD9, CD81, and other tetraspanins ○ Heparin sulfate proteoglycans ○ Integrins and immunoglobulins ○ Lectins
Lipids	• Phosphatidylserine • Sphingoglycolipids • Cholesterol
Nucleic acids	• mRNA • miRNA • other small non-coding RNA

1.4.2. **Classification**

- *Exosomes* (~ 50 – 150 nm): produced through the endocytic pathway, by inward budding of endosomal compartments, called multivesicular bodies (MVB), which were formed by invagination of the cell membrane. The release of the exosomes into the extracellular environment is done by fusion of the MVB with the plasma membrane (Tannetta, Masliukaite et al. 2016). For years, it was described that exosomes had a cup-shaped appearance when seen through transmission electron microscopy; but, when observed by Cryo-Electron Microscopy, exosomes present a rounded shape, evidencing that their early descriptions contained artifacts of the fixation/contrast step, which induced shrinking of subcellular structures (Colombo, Raposo et al. 2014). Exosomes contain endosomal membrane markers (Tetraspanins: CD63, CD9, CD81, TSG101, and Alix) (Escudero, Herlitz et al. 2016); RNA species (miRNA, other non-coding RNA, and coding RNA); and are highly enriched in glycosphingolipids, cholesterol, and phosphatidylserine.

- *Microvesicles* (~ 100 – 1,000 nm): released directly from the plasma membrane to the extracellular space by its outward blebbing (Tannetta, Masliukaite et al. 2016). Their lipid composition is similar to the plasma membrane, occurring selectively in the lipid-rich microdomains of the membrane. They are also enriched with CD40, MMP2 and CK18 protein markers (Escudero, Herlitz et al. 2016).

- *Apoptotic bodies* (~ 200 – 5,000 nm): origin from cells undergoing programmed death (Tannetta, Masliukaite et al. 2016). Studies in apoptotic bodies indicate that they are enriched in histones and fragmented DNA, and also contain cellular organelles and cytosolic components (Escudero, Herlitz et al. 2016).

Table 2. Classification of EVs based on their biogenesis

	Size (nm)	Biogenesis	Membrane Markers (most common)
Exosomes	50 – 150	Endocytic pathway	CD63 CD81 CD9
Microvesicles	100 – 1,000	Directly from the plasma membrane	CD40 MMP2 CK18
Apoptotic Bodies	200 – 5,000	Cell fragmentation	-

1.4.3. Experimental modification of miRNA content in EVs

The analysis of the composition of EVs has been done to demonstrate that they are an actively released particle of the cell, rather than debris. Some techniques, like proteomic analysis, showed that their production and secretion depend on specific stimuli but do not occur randomly (Thery 2011). The expression of nucleic acids in EVs indicates their involvement in cell-cell communication. Generally, EVs are enriched mostly with small RNAs, characterized by multiple techniques, being qPCR one of them (Abels and Breakefield 2016). It has been shown that MV- and EXO-enriched fractions from miR-141-mimic transfected cells expressed elevated miR-141 levels when compared with their respective controls (Ospina-Prieto, Chaiwangyen et al. 2016) (Figure 3).
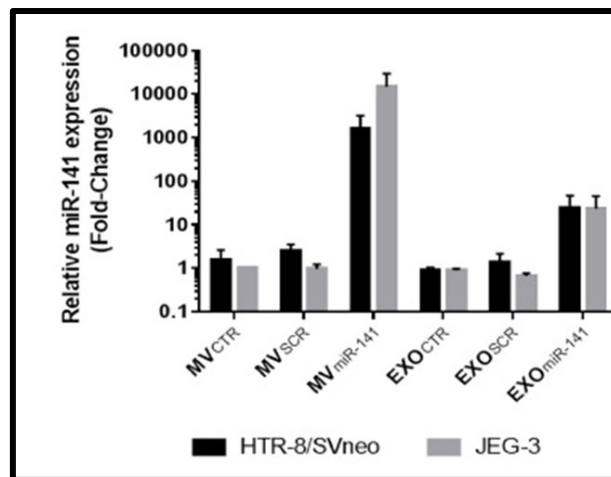

Figure 3. miR-141 expression in particles isolated from the supernatant of trophoblastic cells. Analysis by qPCR of miR-141-containing EVs isolated from transfected cells shows higher expression when compared with their respective controls. Taken from (Ospina-Prieto, Chaiwangyen et al. 2016).

2. HYPOTHESIS AND OBJECTIVES

2.1. Hypothesis

miR-141 is up-regulated in preeclampsia and controls viability and invasion of trophoblast cells. It belongs to the family of miR-200, which has been associated with angiogenesis in other cellular models. Because improper trophoblast ability to remodel HUVEC has been reported in preeclampsia, it is to hypothesize that miR-141 plays an important role in the vascular tube-like formations by regulating trophoblast-endothelial cell interaction. Likewise, secretion of miR-141 in EVs may be involved in the angiogenesis dysregulation observed in preeclampsia.

2.2. Objectives

2.2.1. General

To investigate the function of miR-141 on the trophoblast-endothelial cell interaction in a 3D model that resembles angiogenesis in normal and preeclamptic pregnancies.

2.2.2. Specific

- To establish a 3D co-culture model that allows quantification of trophoblast (HTR8/SVneo and JEG-3) and endothelial (HUVEC) cell interaction.

- To modify the levels of miR-141 expression in trophoblastic cells and to investigate its effects in co-culture with HUVEC.

- To isolate and characterize EVs containing elevated miR-141 levels.

- To investigate the effect of miR-141-containing EVs on the endothelial tube formation.

3. MATERIALS AND METHODS

3.1. Cell Lines

3.1.1. HTR8/SVneo

This cell line was kindly provided by C. H. Graham; Kingston, Canada. HTR8/SVneo cells were derived from human first-trimester trophoblast cells, which were immortalized by transfection with a plasmid containing the gene for the simian virus 40 large T antigen. These cells retain many of the phenotypic features of the parental cells and provide a model of placental functions (Graham, Hawley et al. 1993).

3.1.2. JEG-3

(DSMZ, Braunschweig, Germany); JEG-3 cells are an adherent human choriocarcinoma cell line, originally established by Kohler and Bridson, that preserves several third-trimester trophoblast-like capacities (Kohler and Bridson 1971). Both, the JEG-3 and the HTR8/SVneo cells, are frequently used as models of physiologically invasive EVT (Salomon, Yee et al. 2014).

3.1.3. HUVEC

(DMSZ, Germany); HUVEC are isolated cells from the vein of the umbilical cord, and are considered 'primary' cells because they have been preserved after only 1 to 3 passages from the initial source material (ATCC), and maintained in culture for experiments until passage 10. They are commonly used as a cell model system for the study of various physiological and pathological processes involving endothelial cells.
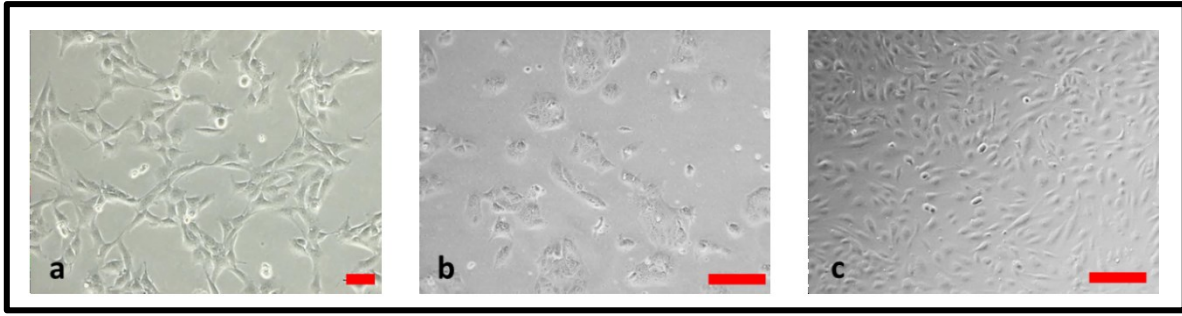
Figure 4. Cell lines in monolayer culture. (a) HTR8/SVneo cells (b) JEG-3 cells (c) HUVEC. Red line indicates 10 μm.

3.2. Cell Culture Conditions

Cells were seeded at 10^6 cells in 75 cm^2 flasks and maintained under standard culture conditions: 37 °C and humidified under an atmosphere of 5% CO_2-balanced N_2 to obtain 8% O_2 (pO$_2$ ~ 54 mmHg). JEG-3 cells were cultured in Ham's F-12 Nutrient Mix (Gibco®, Paisley, UK) and HTR8/SVneo cells in RPMI 1640 Medium (Gibco®), both mediums supplemented with 10% Fetal Bovine Serum (FBS; Sigma-Aldrich, Germany) and 1% Penicillin-Streptomycin antibiotic solution (Gibco®). HUVEC were seeded in Endothelial Cell Growth Medium (ECGM; PromoCell, Heidelberg, Germany) supplemented with 10% FBS and Supplement Mix (PromoCell). All cell lines were routinely tested to confirm the absence of *Mycoplasma*.

3.3. Transfection

Trophoblastic cells were cultured in 6-well plates and allowed to attach overnight, and used after reaching 40 – 60% of confluence. To overexpress miR-141, cells were transfected with miR-141-mimic (mirVana® miRNA mimic, Ambion). To suppress native miR-141 expression, JEG-3 cells were transfected with miR-141 inhibitor (ThermoScientific, Dharmacon). In order to assess the specificity of the transfection with miR-141-mimic or –inhibitor, cells were transfected with non-genomic scrambled sequences, labeled respectively as SCR-mimic (mirVana[TM] miRNA mimic negative control #1; Ambion) and –inhibitor (mirVana[TM] miRNA inhibitor negative control #1; Ambion). All the sequences were transfected at a final concentration of 25 nM using oligofectamine transfection reagent (Oligofectamine[TM] Reagent, Invitrogen, California, USA) according to the manufacturer's

recommendations. Cells were seeded in reduced serum media OPTI-MEM$^®$ I + GlutaMAX^{TM} –I (Gibco$^®$) and 4 h after incubation with sequences, medium containing 30% FBS Exosome-Depleted (Gibco$^®$) was added and left overnight. To minimize toxicity, the used medium was replaced at the next day with 5 ml of medium containing 10% FBS Exosome-Depleted.

3.4. Tube Formation Assay

3.4.1. Initial protocol

Day 1

Corning® Matrigel® Basement Membrane Matrix Growth Factor Reduced (GFR; Corning, Bedford, MA, USA) is a solubilized basement membrane preparation extracted from the Engelbreth-Holm-Swarm (EHS) mouse sarcoma, a tumor rich in extracellular matrix proteins. It was previously thawed (from −20 °C) by leaving it overnight at 4 °C and kept on ice because it gels above 10 °C. CultureSlides (BD Falcon, NY, USA) and pipettes tips were pre-cooled at -20 °C. CultureSlides were coated with 250 µl Matrigel, avoiding air bubbles, and incubated at 37 °C for 30 min to allow solidification. The wells were later filled up with 1 ml of supplemented ECGM and incubated at 37 °C overnight.

Day 2

Staining was done using CellTracker™ Green CMFDA Dye (Life Technologies, OR, USA), beforehand dissolved in Dimethyl Sulfoxide (DMSO) to a final concentration of 10 mM. The stock solution was diluted in serum-free medium to obtain a working solution of 10 µM. This working solution was added to 5 x 10^5 HUVEC in a 25 cm^2 flask and incubated for 30 min at 37 °C. CellTracker™ solution was then removed; cells were washed three times with phosphate-buffered saline (PBS), detached with Trypsin/EDTA and seeded on Matrigel-coated CultureSlides (100,000 cells/ml of new supplemented medium). Cells in CultureSlides were incubated overnight at 37 °C for tube formation.

Day 3

Used ECGM was removed, cells were washed with PBS, and 500 µl of supplemented ECGM was added. Transfected trophoblastic cells were stained with CellTracker™ Orange CMTMR Dye (Life Technologies, OR, USA) diluted in their corresponding serum-free medium, using the same procedure as for HUVEC. 100,000 stained cells in 500 µL of the corresponding supplemented medium were added to the CultureSlides, having a total of 1 ml combined medium in the CultureSlides.

Day 4

After removing medium from CultureSlides, cells were washed carefully with PBS and fixed by adding 1 ml of Methanol/DMSO (4:1) for 24 h at 4 °C.

Day 5

Methanol/DMSO was removed; chamber washed with PBS, and plastic cover from the chambers was detached. VectaShield® (Vector Laboratories, CA, USA), a mounting medium for fluorescence was added. A coverslip was carefully placed over the slides and sealed with nail polish to avoid detachment of the coverslip. Changes in the tube formation were observed and images were taken at low magnification (50x) using an Olympus IX-81 inverted system microscope (Olympus Europe Holding, Hamburg, Germany).
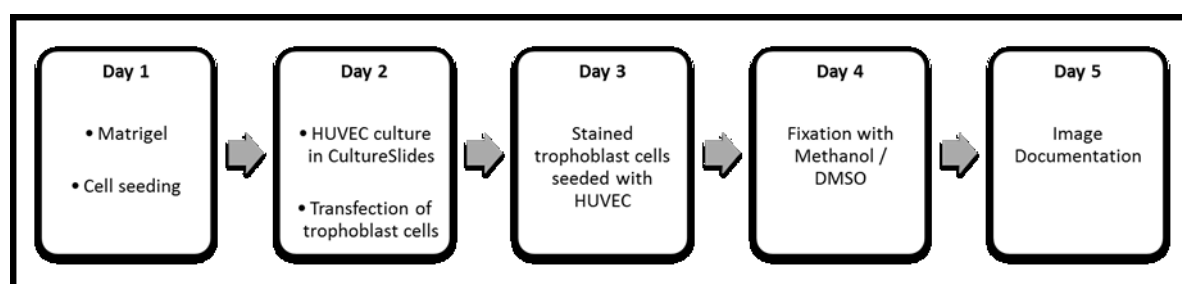

Figure 5. Experimental design for the tube formation assay in CultureSlides. Preparation and culture in a 5-day experiment, summarizing the steps day by day.

This initial protocol had several disadvantages, such as the high number of HUVEC required, their short lifespan in culture, and the amount of Matrigel (250 µl per chamber, 6 chambers) per experiment. Therefore, part of this study was to improve this method to reduce experimentation time and costs.

3.4.2. Optimized protocol

Day 1

Corning® Matrigel® Basement Membrane Matrix GFR Phenol Red Free (Corning, Bedford, MA, USA) was thawed from −20 °C by leaving it overnight at 4 °C and kept on ice. μ–Plate Angiogenesis 96Well, ibiTreat (ibidi, Munich, Germany) were coated with 10 µl Matrigel, avoiding air bubbles, and incubated at 37 °C for 30 min to allow solidification. Thereafter, wells were filled up with 50 µl supplemented ECGM and incubated overnight.

Day 2

5×10^5 HUVEC in a 25 cm^2 flask were stained for 30 min at 37 °C with CellTracker™ Green CMFDA dye (Excitation 492 nm, Emission 517nm) diluted in serum-free ECGM at a final concentration of 10 µM. After CellTracker™ solution was removed; cells were washed, seeded at 6,500 cells per well and incubated at 37 °C for at least 4 h for tube formation. During that time, trophoblastic cells were stained with CellTracker™ Orange CMTMR (Ex. 540 nm, Em. 565 nm) dye diluted in their corresponding serum-free medium, using the same procedure as with HUVEC. Trophoblastic cells were seeded on the HUVEC tube formation trying not to touch the gel matrix with the pipet tip. Excitation and emission values referred above as the absorption and fluorescence emission maxima of the respective fluorescent dyes.

Day 3

After 20 h of co-culture, changes in the tube formation were observed and pictures were taken at low magnification (50x) using an Olympus IX-81 inverted system microscope. Fixation was not needed. Each tube formation assay was performed in at least three independent experiments using minimum three Matrigel-coated wells per condition and one picture per well, with each filter, FITC and TRITC, and the merge of both images. FITC filter for the green fluorescent dye applied to HUVEC (Ex. 463 – 500 nm, Em. 516 – 556 nm) and TRITC filter for the red fluorescent dye applied to trophoblastic cells (Ex. 532 – 544 nm, Em. 573 - 613 nm).
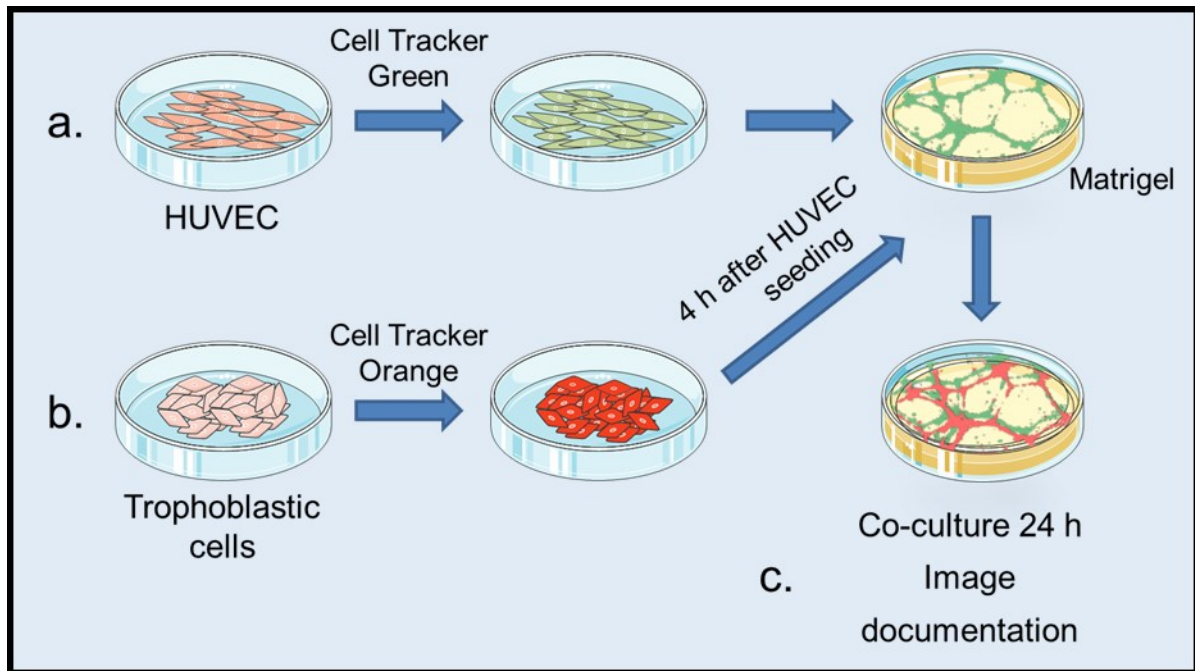
Figure 6. Experimental design for the tube formation assay in µ–Plate Angiogenesis 96Well. a) HUVEC were stained with a green fluorescent dye (Cell Tracker Green) and later seeded on Matrigel. b) Trophoblastic cells were stained with an orange fluorescent dye (Cell Tracker Orange) and co-cultured with HUVEC, which after 4 h presented vascular tube-like formations on Matrigel. c) After 24 h of co-culture incubation, image documentation was done with an inverted fluorescence microscope.

3.5. ImageJ Analysis

The tube formation assay was evaluated using the Angiogenesis Analyzer plugin developed by Carpentier (Gilles Carpentier. Contribution: Angiogenesis Analyzer. ImageJ News, 5 October 2012), implemented in the software ImageJ from the National Institutes of Health, Maryland, USA. Both, the Angiogenesis Analyzer plugin and ImageJ are free downloadable data processing programs that quantify different parameters such as the length of tubes, segments, and nodes (branching points), appreciated in different colors on the final network analysis (c, Figure 7). The pictures from the merged filters were used for the analysis because they showed better the interaction between both cells types. Before analysis, images were changed to an 8-bit format and then to a binary tree format (b, Figure 7). Mean numbers of nodes between tubes were calculated, defining a node as the single point formation when at least three cells are connected (seen in red in (c), Figure 7).
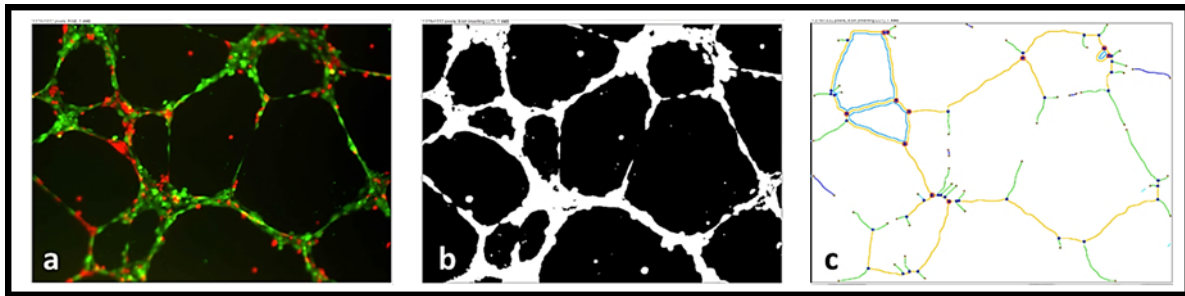
Figure 7. ImageJ Angiogenesis Analyzer. (a) Original merged image, HUVEC (green) and HTR8/SVneo cells (red). (b) Binary Tree. (c) Network Analysis. Red points: nodes, green: branches, yellow: master segments, blue: isolated elements.

3.6. Extracellular Vesicle Isolation

The isolation of enriched-EV fractions (MVs and EXOs) was performed using consecutive centrifugation steps as published by Thery et al. (Thery, Amigorena et al. 2006) (Diagram as Figure 8). Five ml of the conditioned medium was collected 24 h after transfection and centrifuged for 10 min at 380 x g to remove cellular debris. The supernatant was changed to a new tube (Ultra Clear Centrifuge Tubes, Beckman Coulter, California, USA) and ultracentrifuged for 10 min at 10,000 x g to remove apoptotic bodies. The supernatant was removed, placed into a new tube, and ultracentrifuged at 18,890 x g for 30 min. These pellets were washed in PBS, ultracentrifuged again at 18,890 x g for 30 min, and resuspended in 150 µl of PBS to obtain a MV-enriched pellet. Meanwhile, the supernatant was filtrated through 0.8/0.2 µm pore-size filters (Acrodisc® Syringe Filters with Supor® Membrane, Cornwall, UK) and ultra-centrifuged at 100,000 x g for 70 min. The supernatant was removed; the pellet was washed with PBS and ultracentrifuged again at 100,000 x g for 70 min to obtain the exosome-enriched fraction. Pellets were resuspended in 150 µl of PBS. Both pellets (EXO and MV) were stored at -80 °C until further analysis.
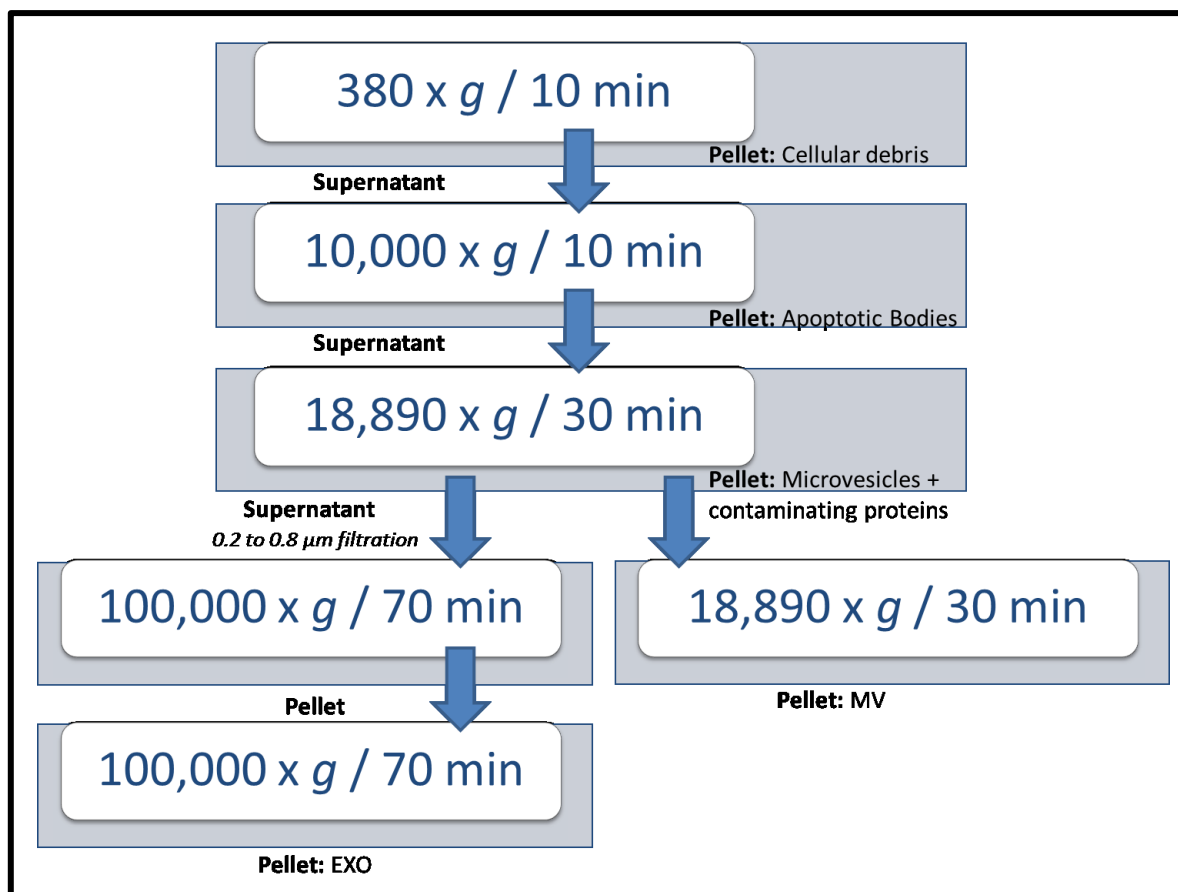
Figure 8. Experimental design for EVs isolation. EXO- and MV-enriched fractions obtained by consecutive centrifugation steps.

3.7. Nanoparticle Tracking Analysis (NTA)

For size distribution and quantification, the EV-enriched fractions were analyzed using NTA with a NanoSight LM10 software version 2.3 (NanoSight Ltd., Amesbury, UK). The NTA instrument consists of a laser beam that illuminates particles in suspension, a microscope connected to a camera, a hydraulic pump and a measuring chamber (Szatanek, Baj-Krzyworzeka et al. 2017). The light scattered by each particle is focused by the microscope into the camera, which identifies them individually, being tracked and recorded over a certain period of time (Malloy 2011) (Figure 9). Based on their Brownian motion, the software calculates the size and number of particles (Gardiner, Ferreira et al. 2013). The isolated EVs were diluted 1:10 in PBS before analysis, and introduced into the sample chamber at room temperature (RT; 22.7 ± 0.23° C) using 1 ml syringes, washing the chamber with PBS between samples. It was recorded, for each sample, a thirty-seconds video and analyzed using optimized instrument settings (detection threshold: 10; settings

were optimized and kept constant between samples). Values were expressed as means of 3 isolated populations.
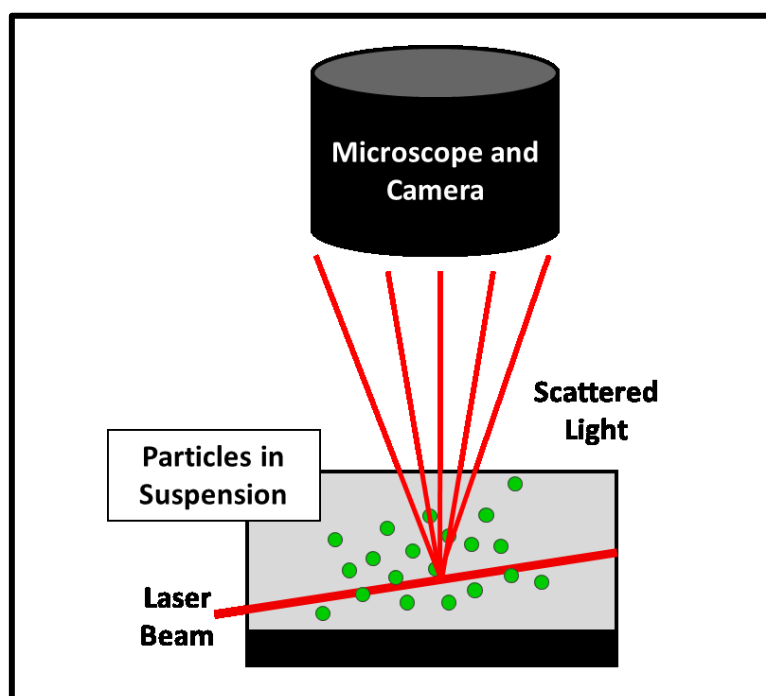
Figure 9. Nanoparticle Tracking Analysis. The laser beam illuminates the particles in suspension, and the scattered light is focused by the microscope into the camera that tracks each particle based on their Brownian motion.

3.8. Dot-Blot

A nitrocellulose membrane was prepared according to the number of samples. 1µl of each sample was dotted into the membrane and left until dry and blotting was repeated for 3 more times. Previously prepared Tris-Buffer Saline (TBS) mixed with 0.05% Tween20 (TBS-T) was used to prepare blocking solutions in combination with free-fat milk. TBS-T 5% milk for 30 min at RT was used to immerse the nitrocellulose membrane and block non-specific sites. The primary antibody anti-human CD63 (ImmunoTools, Germany), in a dilution of 1:500 (in TBS-T 1% milk) was incubated with the membrane at RT for 3 h. The membrane was later washed with TBS-T three times, once for 10 min, and twice for 5 min. The secondary antibody (anti-mouse) conjugated with HRP (Cell Signaling Technology) in a dilution of 1:5,000 (in TBS-T 1% milk) was incubated with the membrane at RT for 1 h. The membrane was later washed with TBS-T three times, 5 min each, and with TBS once for 10 min. Incubation of the membrane was done with 500 µl of Luminata^{TM}

Forte Western HRP Substrate (Millipore; MA, USA) and acquisition of the digital image was done on the ChemiBIS gel documentation system, with different times of exposure (1, 5, 10 and 15 minutes).

3.9. Co-Incubation of Non-Transfected Trophoblastic Cells with Isolated EVs

μ–Plate Angiogenesis 96Well were coated with 10 μl Matrigel. HUVEC were stained with 10 μM CellTracker™ Green CMFDA Dye and non-transfected HTR8/SVneo cells, with CellTracker™ Orange CMTMR Dye in the same procedure as detailed in the tube formation assay method (modified protocol, Figure 6). EVs from cells transfected with miR-141-mimic or controls were added at a concentration of 100 μl/ml. After 18 - 20 h of co-culture incubation at 37 °C and 5% CO_2, changes in the tube formation were observed and pictures were taken at 50x magnification using Olympus IX-81. Each tube formation assay was performed as three independent experiments using at least two wells per condition, with the two different groups of EVs population (EXO and MV).

3.10. Statistical Analysis

Data are expressed as mean ± standard error of the mean (SEM), performed using a commercially available package (Prism 6, GraphPad Inc, CA, USA). Statistical significance ($p < 0.001$) of miR-141 effects in HTR8/SVneo cells was determined using one-way ANOVA with Turkey correction. Statistical significance of miR-141 effect in JEG-3 cells, comparison of the mean size and concentration of EVs, and analysis of EVs containing miR-141 ($p < 0.05$) was determined using two-way ANOVA with Turkey multiple comparison test.

4. RESULTS

4.1. Experimental Design of Angiogenesis Assays

Experiments were done according to protocols previously established in our laboratory. For each experiment, slides with 4 culture chambers were used. Three different conditions and their respective duplicates were established: non-modified cells as a control (CTR), non-genomic scrambled sequences (SCR-mimic and –inhibitor, with JEG-3) and miR-141-mimic and -inhibitor. Images were taken from four different fields per chamber, excluding extreme edges due to gel meniscus formation. Initial pictures have shown a not evaluable merge of colors. Therefore, there were done changes on the initial protocol. The conventional Matrigel GFR was changed to a Phenol-Free Matrigel GFR, reducing possible interference with the fluorescent staining on cells. A "µ–Plate Angiogenesis 96Well", from Ibidi, was applied. The bottom of each well provides an internal flat well for a 10 µl volume of Matrigel and a total medium volume of 50 µl per well. Taking pictures did not further need fixation; as a result, experiments were limited to 3 days. With these changes, clearer images were obtained compared to the initial protocol (Figure 10).

Consequently, the reduction of the seeding area led to changes in the number of cells. For HUVEC, less than 5,000 cells resulted in incomplete or definitely no tube formations; and 10,000 cells led to overlapping formations, deciding the amount of 6,500 cells of each cell line, per well.

It was also seen that by applying the initial protocol, HUVEC died within 48 h in Matrigel (Figure 11). Therefore, culture-steps were also modified. It has been reported that, depending on the cell type, the peak of tube formation may occur between 3 and 12 h, tubes begin to deteriorate within 18 h and endothelial cells undergo apoptosis (DeCicco-Skinner, Henry et al. 2014). HUVEC formed tubes in Matrigel 4 h after seeding, time taken to start co-culture with trophoblastic cells. After 24 h of co-culture incubation, image documentation was done with an inverted fluorescence microscope.
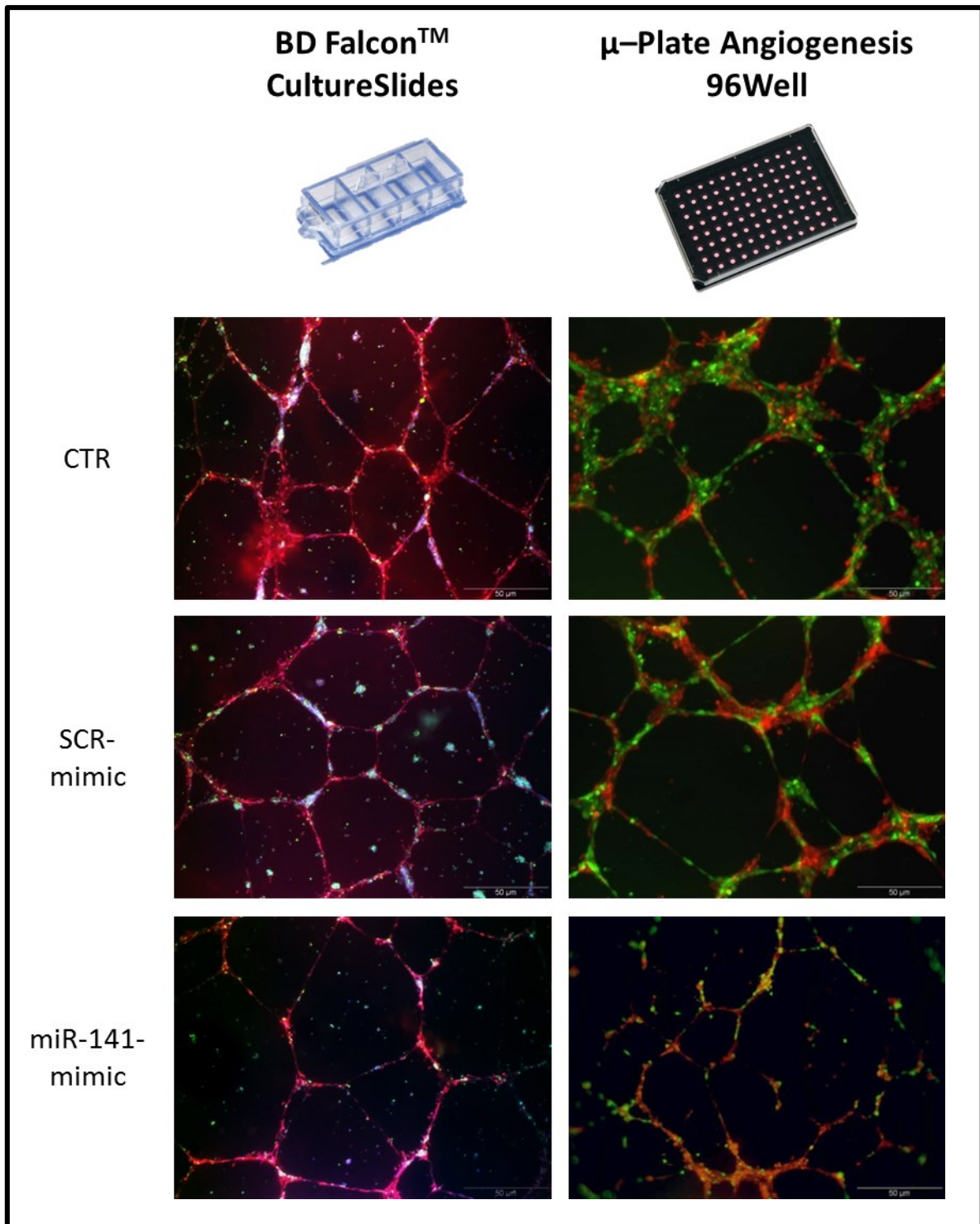
Figure 10. Comparison between CultureSlides and µ–Plate Angiogenesis 96Well. The different cell lines were better distinguished between them by using the 96 well plates when compared with the culture slides. In the 96 well plates, HUVEC are shown in green and HTR8/SVneo cells in orange.
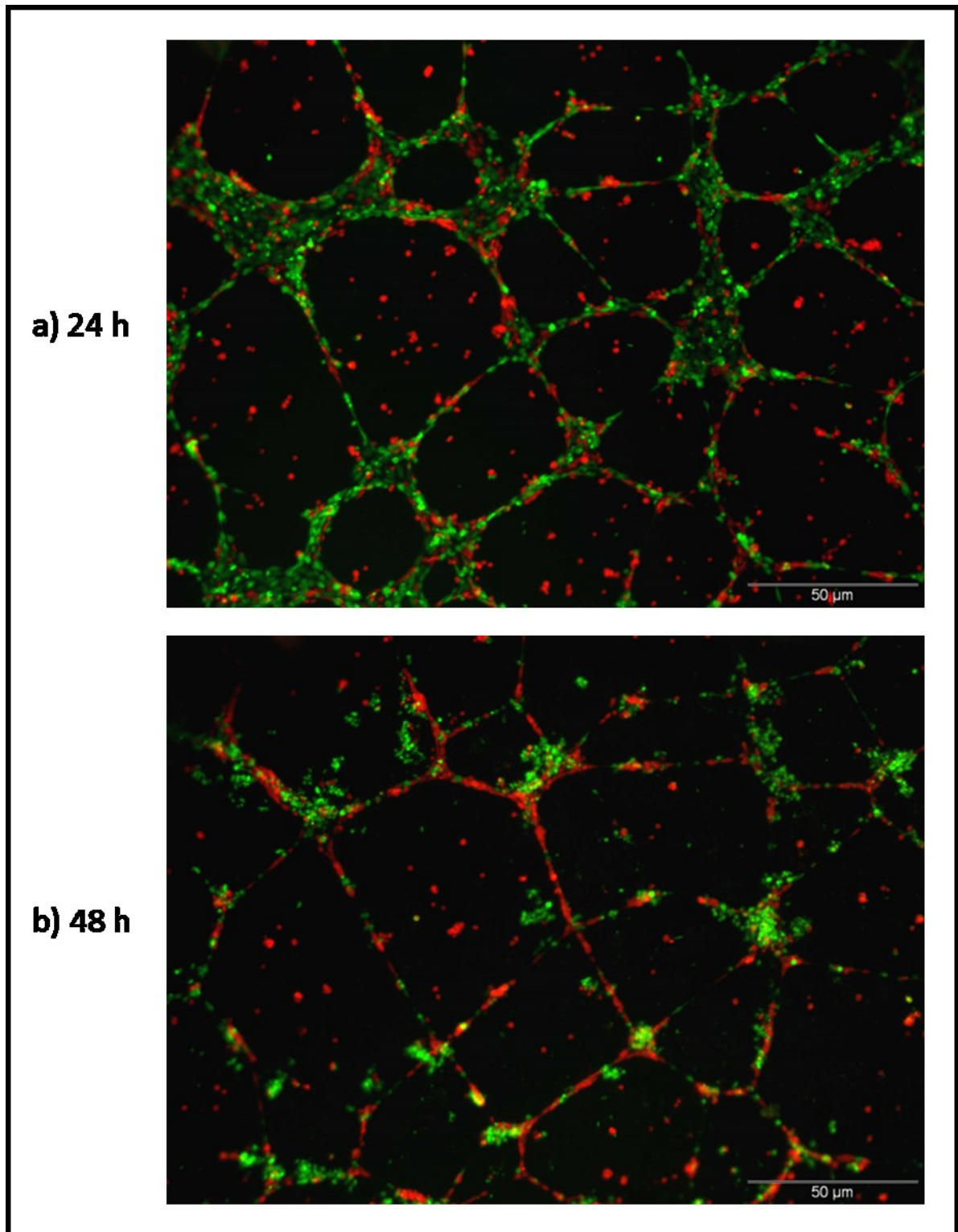
Figure 11. Tube formations after 24 and 48 h of HUVEC in Matrigel. a) HTR8/SVneo cells (orange) were seeded after 24 h HUVEC (green) incubation. The picture was taken after 6 h of co-culture. b) HUVEC after 48 h in Matrigel showed apoptotic cells.

4.2. Cell Lines and Matrigel

Cell growth in Matrigel differs between cell lines. HUVEC formed tubes within 4 h after culture in Matrigel. There was no tube formation in culture of JEG-3 cells. HTR8/SVneo cells showed different results: in some experiments, they tended to organize themselves in small groups, but in other experiments, they displayed a tube formation, as seen in Figure 12. This showed that HTR8/SVneo cells display an "endothelial-like" formation when seeded in Matrigel, which may take relevance in further experiments.
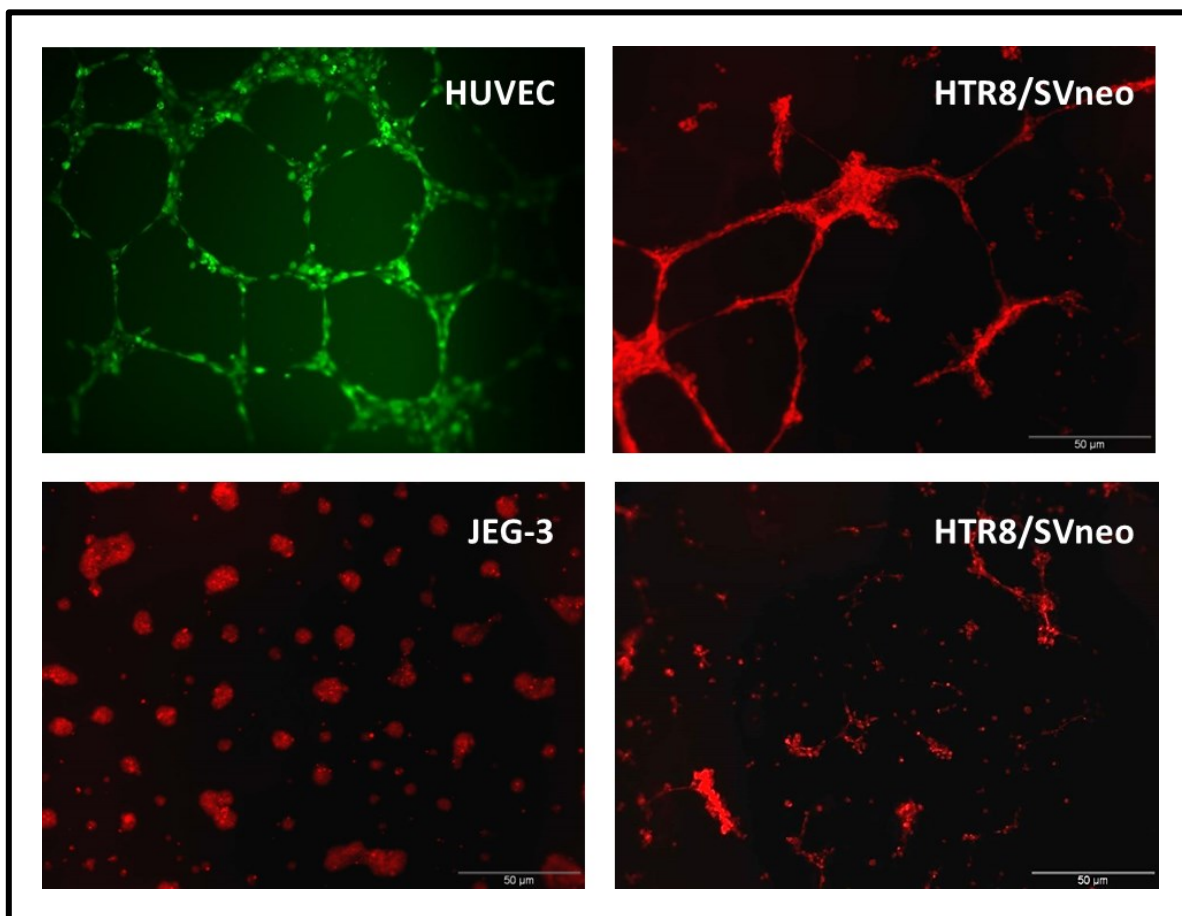

Figure 12. Cell lines cultured in Matrigel. HUVEC's usual tube formations; JEG-3 cells never showed this organization. In contrast, HTR8/SVneo cells have the faculty of forming tubes, but not seen in every experiment.

4.3. Endothelial and Trophoblastic Cell Interaction

HUVEC seeded in Matrigel have been co-cultured with two different trophoblastic cells: HTR8/SVneo cells, immortalized cells deriving from first-trimester trophoblast cells, and JEG-3 choriocarcinoma derived cells with trophoblast-like abilities. HTR8/SVneo cells co-cultured migrated towards the tube formations previously formed by HUVEC and seemed to grow in between the endothelial cells. This interaction remained even when the endothelial cells were apoptotic, which occurred after keeping the co-culture for more than 48 h, representatively seen in Figure 11. On the other hand, JEG-3 cells interacted poorly with HUVEC, tending to grow over the endothelial formations as filling up space rather than a "replacement" (Figure 13 and 14).
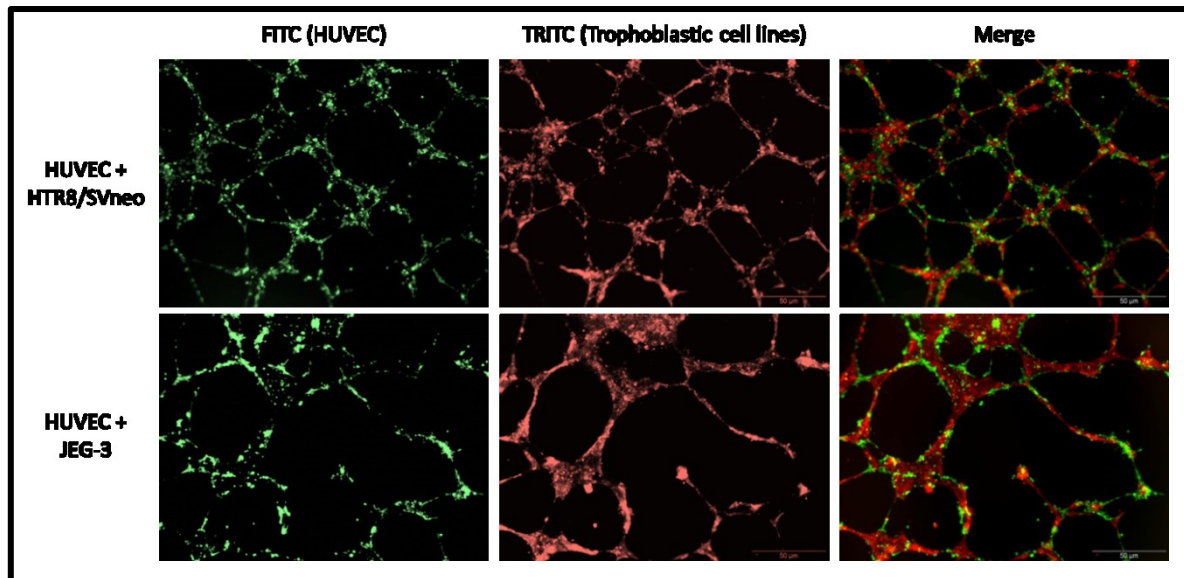

Figure 13. HUVEC co-cultured with different trophoblastic cells. HTR8/SVneo cells seemed to grow in between the endothelial cells in contrast to JEG-3 cells that tend to grow over the endothelial tube formations. FITC, filter used for green-stained HUVEC. TRITC, filter used for red-stained HTR8/SVneo or JEG-3 cells. Merge defined as the combination of both images.
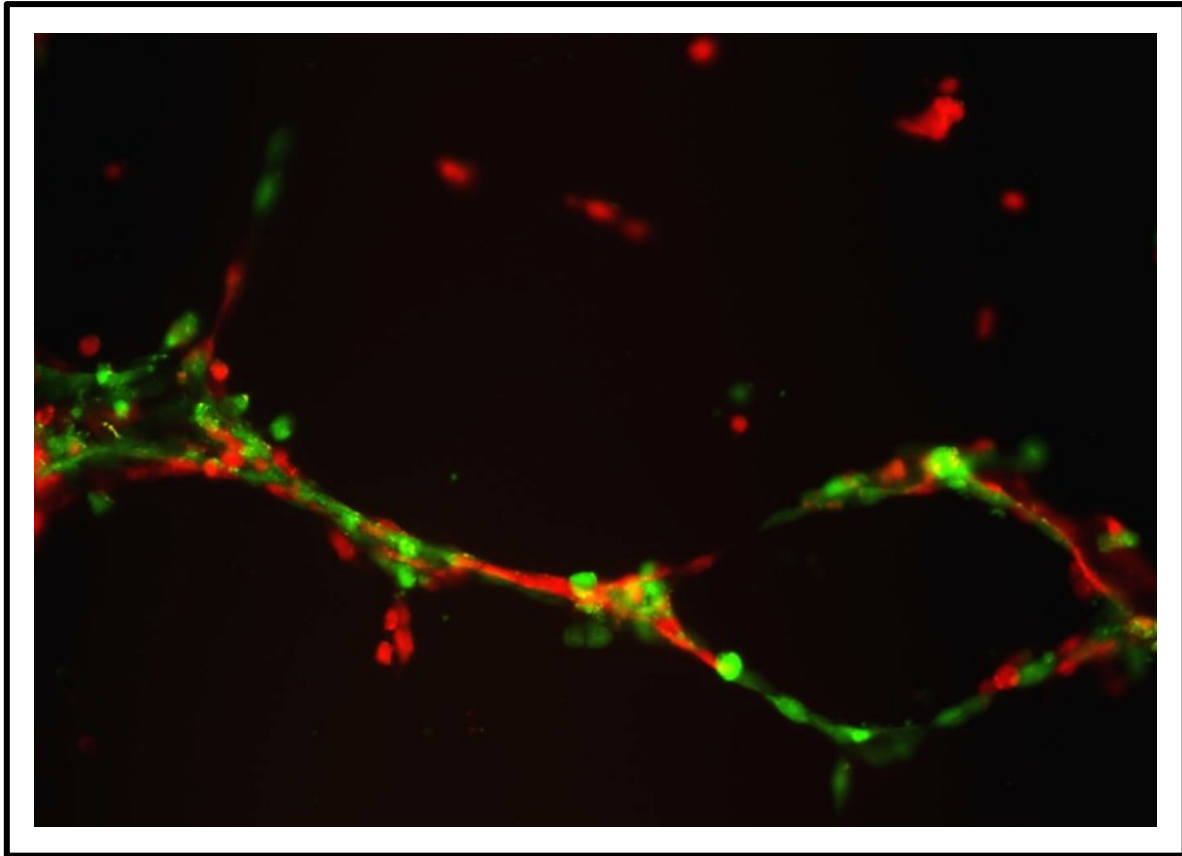
Figure 14. HUVEC and HTR8/SVneo cells interaction. HUVEC were stained with Cell Tracker Green, HTR8/SVneo cells with Cell Tracker Orange. Both cell lines were seeded in Matrigel and picture was taken after 24 h of co-culture, using an Olympus IX-81 at 100x.

4.4. miR-141 Decreases HUVEC-HTR8/SVneo Interaction

The potential influence of miR-141 on the interaction between HUVEC and trophoblastic cells was studied upon modification of its expression in HTR8/SVneo and JEG-3 cells. 20 h after transfection with miR-141-mimic, in HTR8/SVneo cells, a highly significant reduction ($p < 0.001$) of the number of nodes was detectable in comparison to the respective controls transfected with a non-genomic sequence (Figure 15).

In JEG-3 cells, neither overexpression nor inhibition of miR-141 induced a remarkable disruption of the tube formation. The software-driven analysis of nodes presented a slight reduction in the number of nodes, but the differences are not easily distinguishable by eye (Figure 16).
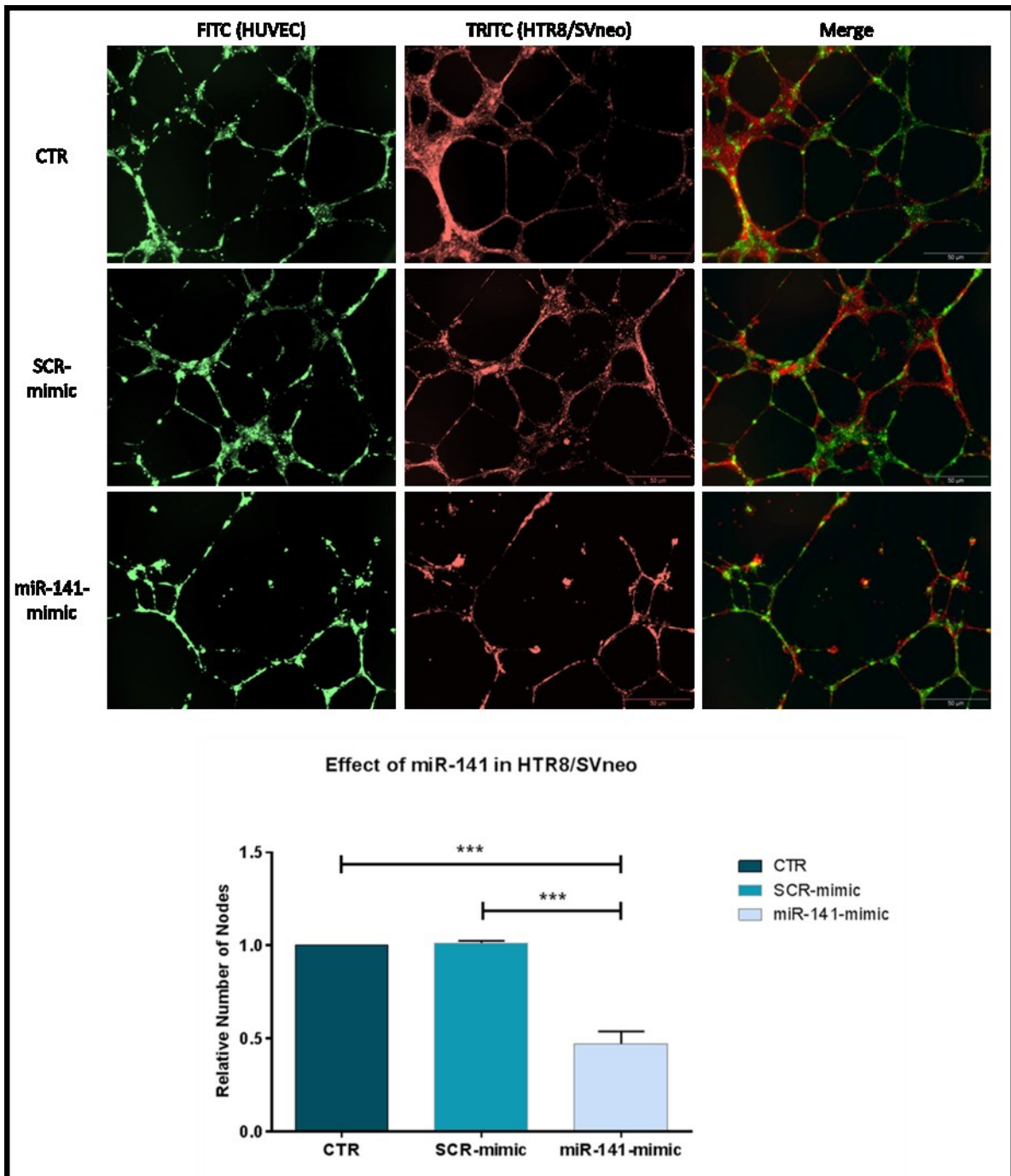
Figure 15. Interaction between HUVEC and transfected HTR8/SVneo cells, and their respective controls. A highly significant reduction (*** $p < 0.001$) of the number of nodes was seen upon overexpression of miR-141. Bars show the mean number of nodes per well normalized to controls (n = 4 experiments based on independent transfections). Error bars show standard error.
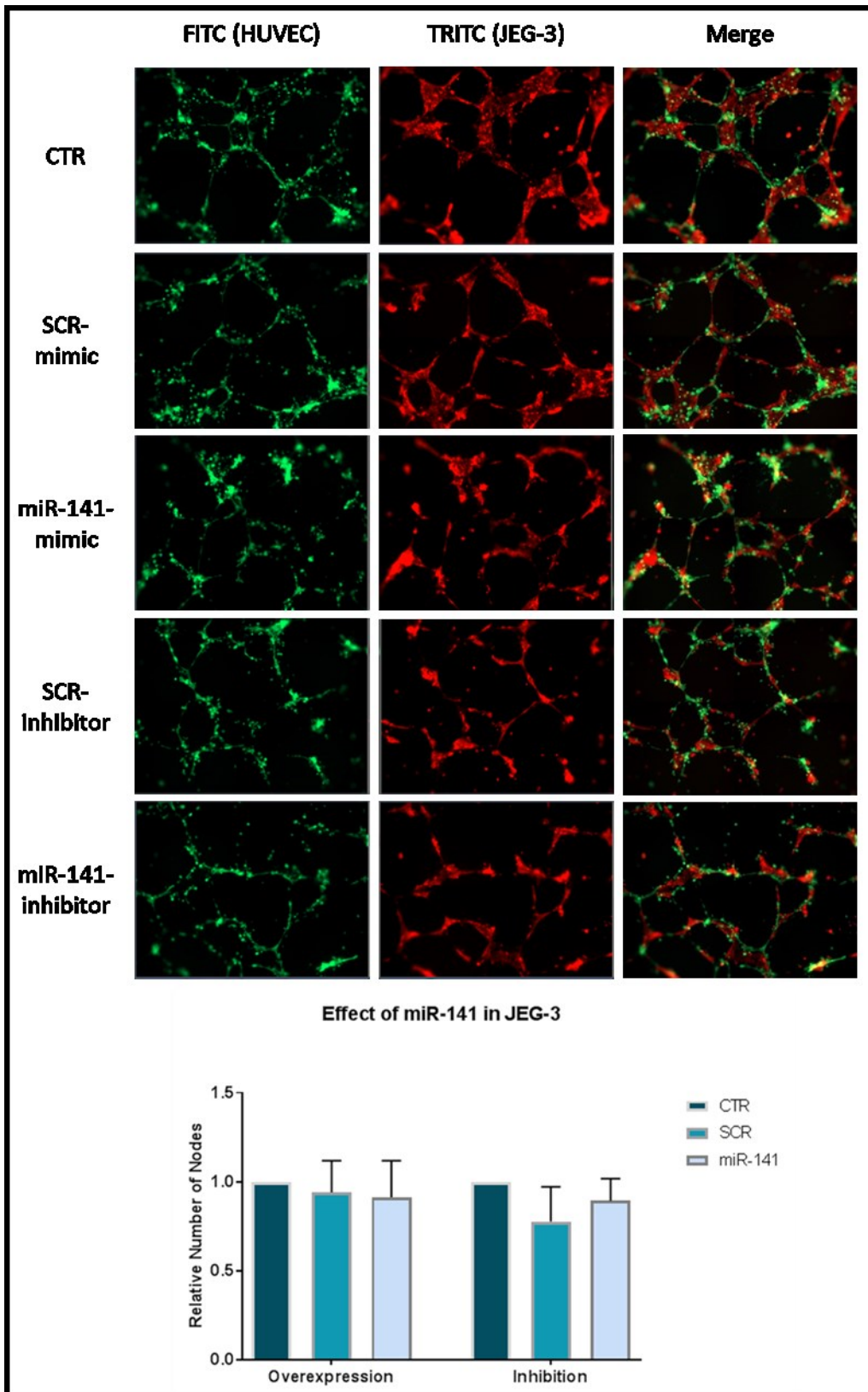
Figure 16. Interaction between HUVEC and transfected JEG-3 cells (overexpression and inhibition of miR-141), and their respective controls. Neither overexpression nor inhibition of miR-141 induced a remarkable disruption of the nodes. Bars show the mean number of nodes per well normalized to controls (n = 3 experiments based on independent transfections). Error bars show standard error.

4.5. Effects of EVs from miR-141-overexpressed Cells on Non-Transfected Cells

4.5.1. Nanosight

After isolation of EVs, an evaluation of their concentration and size of each sample was done by using a NTA system. This method is not highly confident because the size of the particles can be disturbed by the surrounding medium, and because ultracentrifugation only enriches but does not purify them. This means that there may be no complete elimination of larger particles from the resulting sample. Nonetheless, the mean sizes of the enriched fractions, EXO and MV, were near to the expected as seen in Table 3 and Figure 17.

Table 3. Comparison of the mean size of EXO- and MV-enriched fractions produced by HTR8/SVneo cells as assessed by NTA. (n = 3 experiments based on independent transfections). Data are expressed as mean ± SEM.

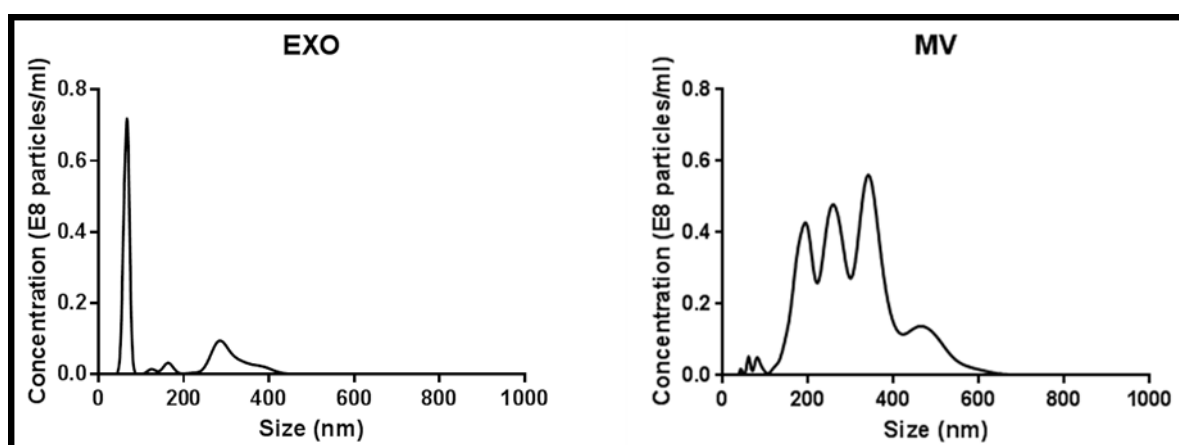|	Size (nm)
EXO	157.1 ± 28.0
MV	258.3 ± 60.2

Figure 17. Representative NTA graph for the size distribution of EXO- and MV-enriched fractions. EVs isolated from HTR8/SVneo cell supernatants were analyzed using a NanoSight LM10 instrument. The curve shows the relative concentration depending on size.

The mean concentration of the EXO-enriched fraction obtained from HTR8/SVneo cells transfected with miR-141-mimic was slightly increased compared with their respective controls. Meanwhile, the mean concentration of the MV-enriched fraction slightly decreased compared with their respective controls (Table 4 and Figure 18).

Table 4. Mean concentration of EVs obtained from HTR8/SVneo cells transfected with miR-141-mimic. (n = 3 experiments based on independent transfections). Data are expressed as mean ± SEM.

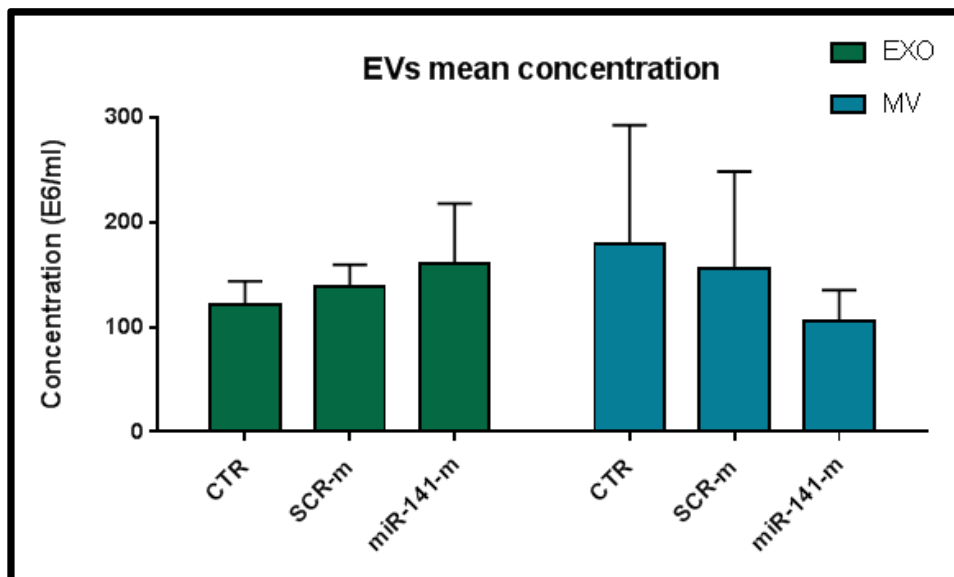|		Particles x 10^6/ml
CTR	EXO	122.2 ± 21.7
	MV	180.0 ± 113.0
SCR-mimic	EXO	138.3 ± 21.7
	MV	156.7 ± 92.2
miR-141-mimic	EXO	161.1 ± 57.0
	MV	105.6 ± 29.9

Figure 18. miR-141 and EVs concentration. Bars show the mean concentration of particles (EXO and MV) obtained from HTR8/SVneo cells transfected with miR-141-mimic. (n = 3 experiments based on independent transfections). Error bars show standard error.

4.5.2. Dot-Blot

Dot Blot is a technique similar to the Western Blot, based to detect proteins but without electrophoretic separation. Because of the small amount of each sample obtained after enrichment through ultracentrifugation, it was taken the decision of using this technique as part of the EV characterization. 4µl per sample showed the presence or not of the protein searched, in this case, the tetraspanin CD63, commonly present on EXOs. Positive signals are found in human platelet and whole cell lysates, used as positive controls. The results showed the presence of the CD63 in cell lysates and blood serum (which contain platelets), and also in the EXO-enriched samples (Figure 19).
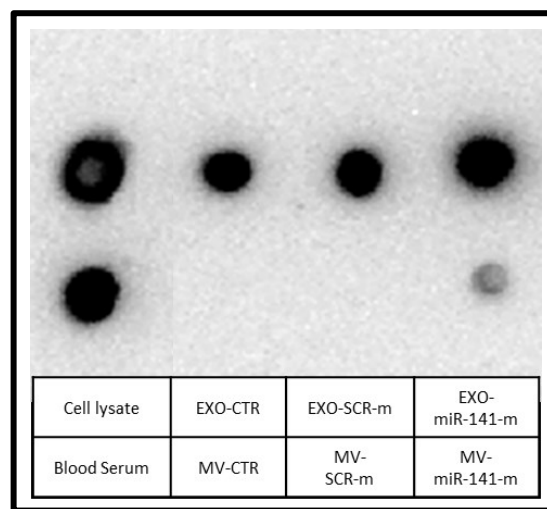
| Cell lysate | EXO-CTR | EXO-SCR-m | EXO-miR-141-m |
| Blood Serum | MV-CTR | MV-SCR-m | MV-miR-141-m |

Figure 19. CD63 presence in EXO- and MV-enriched fractions evaluated through Dot-Blot technique. EV-enriched samples were used to observe the presence of CD63 which is found on human cellular membranes and also on exosomes.

4.5.3. Tube formation

After assessment of the mean concentration of EVs in each sample, it was decided to use a concentration of 100 µl of EVs suspension per 1 ml of culture medium (the equivalent to 10% of the total medium) to study their effects on the tube formations. HUVEC were co-cultured with non-transfected HTR8/SVneo cells, supplemented with MVs or EXOs, obtained from previously treated cells. The tube formation was evaluated by fluorescence microscopy after 20 h of co-culture. Samples supplemented with EXO showed a significant (* $p < 0.05$) decrease of nodes, almost simulating the effect seen when transfected HTR8/SVneo cells were used. Co-cultures incubated with MV showed a slight, but not significant reduction of nodes (Figure 20).
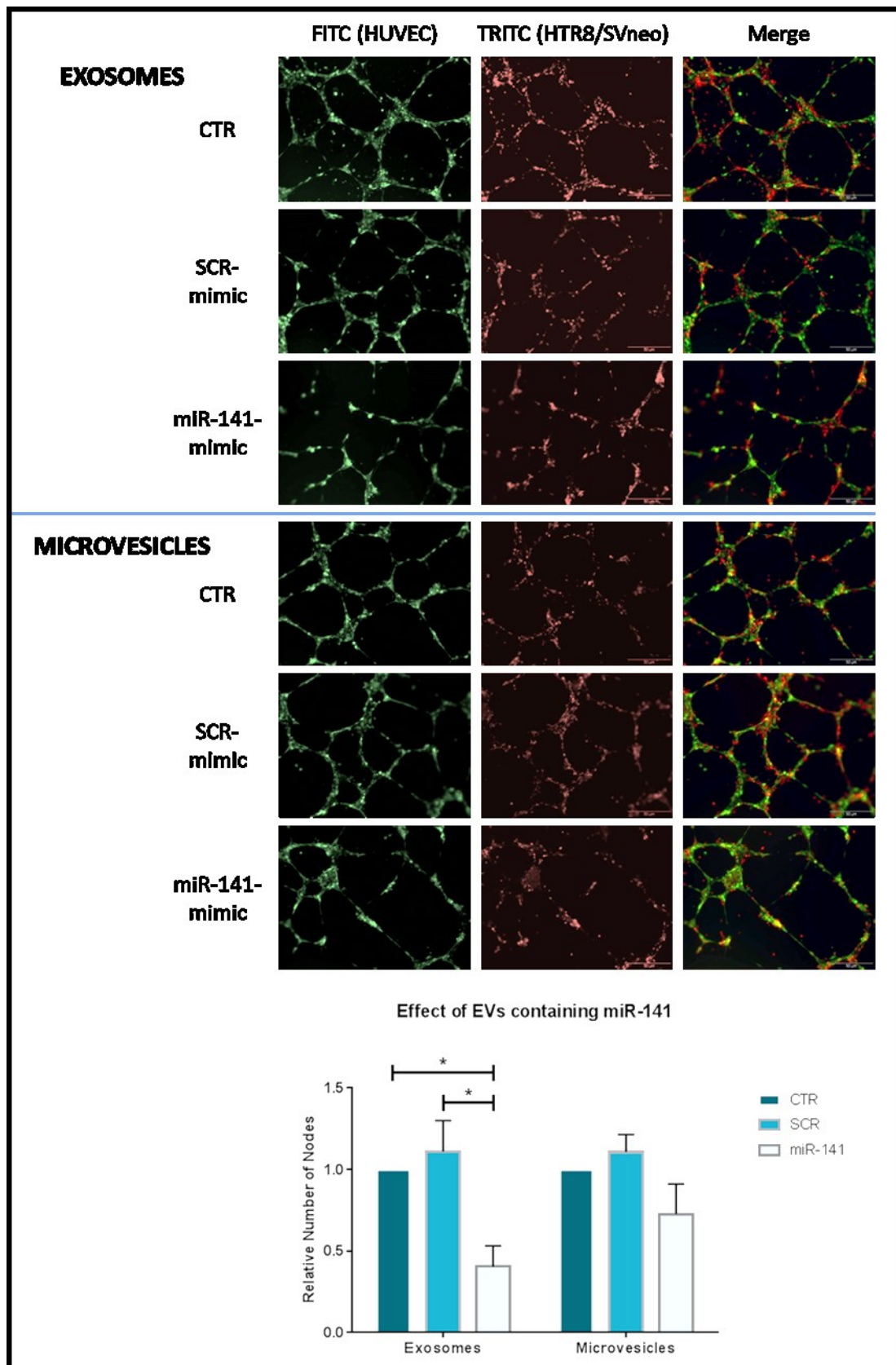
Figure 20. HUVEC co-cultured with non-treated HTR8/SVneo cells and supplemented with EVs from previously transfected HTR8/SVneo cells. Bars show the mean number of nodes per well normalized to control (n = 3 experiments based on independent transfections). Error bars show standard error (* $p < 0.05$).

5. DISCUSSION

5.1. From Physiological Development to a Multisystemic Syndrome

Preeclampsia is a hypertensive disorder diagnosed with the appearance of *de-novo* hypertension and proteinuria. These clinical signs usually appear during the second half of pregnancy, but initial pathogenic mechanisms, which still remain vague, arise much earlier. The lack of evidence about the definitive etiology and the absence of an adequate treatment lead to the increase in maternal and perinatal morbidity and mortality rates around the world (WHO 2011). So far is known, the placenta plays an important role in preeclampsia as the symptoms disappear after delivery. It is also recognized that the clinical symptoms are caused by a dysfunction of the maternal endothelium, a deficient trophoblast invasion and an inadequate remodeling of the uterine spiral arteries (Ahmed and Ramma 2015). These changes fall into the inadequate supply of blood to the developing uteroplacental unit, increasing the risk of fetal growth restrictions or unsuccessful pregnancy outcome caused by endothelial dysfunction (Uzan, Carbonnel et al. 2011).

During the first trimester of pregnancy, the endothelial cells go through differentiation in the later stages of angiogenesis, a process that involves the formation of new blood vessels from previous vascular formations. The endothelial cells degrade the basement membrane, migrate toward an angiogenic stimulus, proliferate and organize themselves in tubular networks (Marquez-Curtis, Sultani et al. 2016). *In vitro,* these tubular networks are studied on a 3D cell culture model based on the patent US 20110059904 A1: *Serum-based, diagnostic, biological assay to predict pregnancy disorders* (Sharma and Kalkunte 2011), that simulates the interaction of fetal trophoblast cells with endothelial cells in response to pregnancy serum. It is grounded on the "cross-talk" between fetal and maternal cells at the fetal-maternal interface and the remodeling of the uterine spiral arteries during trophoblast invasion (Humphries and Yang 2015) (Whitley and Cartwright 2010).

This 3D model uses a Matrigel basement membrane extracted from the EHS mouse sarcoma, a tumor rich in extracellular matrix proteins such as laminin, collagen IV, and heparin sulfate proteoglycans (Kleinman, McGarvey et al. 1982). This Matrigel simulates the extracellular matrix, but with small amounts of growth factors that occur naturally in the EHS tumor such as the epidermal, insulin-like, fibroblast and transforming growth factors, and tissue plasminogen activator (Guidelines for use – Corning ® Matrigel ® Basement Membrane Matrix GFR). By using a Matrigel GFR, stimuli interferences are reduced, and experimental settings are easier to define (DeCicco-Skinner, Henry et al. 2014).

Cell lines frequently used as models of invasive EVT are the immortalized HTR8/SVneo cells that derive from human first-trimester trophoblast cells; and JEG-3 cells, which derive from human choriocarcinoma. Although JEG-3 cells preserve several trophoblast-like capacities, their invasion ability is lower compared to HTR8/SVneo cells (Morales-Prieto, Schleussner et al. 2011) (Suman and Gupta 2012).

HUVEC seeded on Matrigel do not proliferate, but they tend to form tubular formations with an inner lumen (Sokolov, Lvova et al. 2017). HTR8/SVneo cells also create tubes in Matrigel (Highet, Zhang et al. 2012); meanwhile, JEG-3 cells do not show this characteristic. The reason why JEG-3 cells do not have similar capacities in the 3D Matrigel model is not clear. It might be that, due to their malign origin, JEG-3 cells present a less organized growth pattern. It can also be related to different genotype and the phenotype of both trophoblastic cells (Bilban, Tauber et al. 2010).

When seeded in co-culture with HUVEC, HTR8/SVneo cells seemed to reinforce the endothelial tube formations rather than to form further tubes. It has been seen that HTR8/SVneo cells follow the original endothelial tubes, even though HUVEC died within the first 24 h (Aldo, Krikun et al. 2007) (Alvarez, Mulla et al. 2015). *In vivo*, trophoblast cells migrate across the endothelium, adopt an endothelial-like phenotype and coat the lumen within the spiral arteries by replacement of the endothelial cells, which undergo apoptosis (Degner, Magness et al. 2017). *In vitro,* Matrigel induces the HTR8/SVneo cells to differentiate into an invasive EVT

phenotype, and to create vascular tube-like formations by overexpression of *CDH5,* a gene that encodes the Vascular Endothelial Cadherin, also known as VE-cadherin (Highet, Zhang et al. 2012).

When seeded in co-culture with HUVEC, JEG-3 cells grew along the endothelial tubes but did not tend to create connections and did not keep the tube formations after HUVEC apoptosis. This can be probably explained by an impaired cell-cell adhesion due to a deficient expression of adhesion molecules (Bulmer, Burton et al. 2012).

Studies using this 3D *in vitro* assay, with additional treatment of serum from normal and pathological pregnancies, like preeclampsia, described disrupted tube formations of the endothelial cells in co-culture with trophoblasts (Kalkunte, Lai et al. 2009). Previous studies in our lab have shown that miR-141 expression, a placenta-related miRNA, is higher in plasma and placentas from preeclampsia than from normal pregnancies (Ospina-Prieto, Chaiwangyen et al. 2016). Therefore, it was aimed to investigate the role of miR-141 in endothelial tube formation during the trophoblast-endothelial interaction.

5.2. miR-141

Numerous diseases, of very different etiologies, have been related to the dysregulation of miRNAs. miRNAs are short non-coding RNAs (approximately 22 nucleotides in length), which are involved in the post-transcriptional control of gene expression, either by degrading mRNA or by modifying its translation (Gregory and Shiekhattar 2005) (Ha and Kim 2014). An increasing number of studies have suggested also a link between several miRNAs disorders and pregnancy pathologies, such as preeclampsia, and proposed their concentration in plasma/serum as potential biomarkers.

The miR-200 family is known for the regulation of cell migration, invasion, and proliferation; mostly investigated in the field of cancer research. miRNAs belonging to this family have been also identified as endogenous angiogenesis inhibitors. Endothelial tube formations decrease significantly when treated with supernatant from the ovarian cell line HeyA8, which express miR-200a and miR-200b (Pecot, Rupaimoole et al. 2013). miR-141, also part of the miR-200 family, has been studied previously in breast, pancreas, ovary and colon malignancies (Humphries and Yang 2015).

Overexpression of miR-141, as seen in preeclampsia, was done in HTR8/SVneo and JEG-3 cells by transient transfection. The potential effects were analyzed in co-culture with HUVEC on the tube formation assay. The overexpression of miR-141 in transfected HTR8/SVneo cells showed a highly significant ($p < 0.001$) reduction of nodes, suggesting that the overexpression of miR-141 tends to weaken the interactions between these cell lines, which ends in tube rupture. In JEG-3 cells the endogenous expression of miR-141 is higher than in HTR8/SVneo cells (Ospina-Prieto, Chaiwangyen et al. 2016), but miR-141 overexpression and inhibition in this cell line did lead to almost no changes in its interaction with HUVEC. This can be suggested by the fact that the downregulation of miR-141 on JEG-3 cells inhibits their proliferation; while, the overexpression of this miRNA does not affect this cell process (Morales-Prieto, Schleussner et al. 2011).

The applied model has the capability of mimicking insufficient trophoblast invasion followed by reduced tubular formations, which *in vivo* may lead to poor blood supply

as seen during preeclampsia. Results indicate that miR-141 may play a role in the angiogenic potential of HTR8/SVneo cells and their communication with endothelial cells, probably carried out by EVs.

5.3. Extracellular Vesicles

miRNAs can be released into the extracellular space as a cargo of different types of EVs (EXO or MV), protected from RNases and transported in a relatively stable way (Ouyang, Mouillet et al. 2014). EVs are considered important carriers of various proteins, mRNAs, microRNAs and lipids which interact with distant tissues in the body, being involved in the intracellular communication during normal and pathological conditions (Raposo and Stoorvogel 2013). Several studies show the relationship between mother and embryo during the implantation phase, mediated by EVs (Cretoiu, Xu et al. 2016).

Placental miR-141 has been detected in maternal plasma within small particles, which cannot be filtered out, even using 0.22 µm filters in contrast to the placental chorionic somatomammotropin hormone 1 transcript, a placental mRNA (Chim, Shing et al. 2008). To recognize the effect of miR-141-containing EVs, the isolation of particles released from transfected trophoblastic cells was done by differential centrifugation. Larger vesicles can be separated by consecutive centrifugations at increasing speeds, and the small particles (EXO), sedimented at 100,000 x g (Colombo, Raposo et al. 2014).

The collected EVs were characterized by NTA and Dot-Blot technique. The NTA consist of a laser beam sent through a sample suspension; the light scattered by the particles is then directed to a camera attached to a conventional microscope. The software identifies and tracks the Brownian motion of each particle from frame to frame, enabling the calculation of the approximate diameter and the number of particles per ml (Filipe, Hawe et al. 2010). Some results showed that miR-141 may be involved in the particle concentration. The EXO-enriched fraction obtained from HTR8/SVneo cells transfected with miR-141-mimic showed a slight increase compared with its respective controls. Meanwhile, the concentration of MV-enriched

fraction was slightly decreased compared with their respective controls. External factors are involved in EVs release (Abels and Breakefield 2016); in this case, it can be thought that miR-141 may play a role in the production of EVs.

The next characterization step was done by confirmation of membrane proteins with a Dot-Blot technique, which is similar to the Western Blot but without electrophoretic separation. By using a small amount of each EVs sample, it was showed the presence of the tetraspanin CD63 on the EXOs. Together with the CD9, the CD63 is one of the most common tetraspanins involved in exosome formation. The exosomes biogenesis consists in the accumulation of intraluminal vesicles (ILV) inside early endosomes which later mature into late endosomes (referred as MVB) and subsequently secreted (Colombo, Raposo et al. 2014). These ILV are formed by the inward budding of the MVB which contain specific proteins, lipids, and other components.

After obtaining information about enriched EXO- and MV-fractions, it was evaluated the interaction between HUVEC and EVs. EVs from the plasma of women with preeclampsia cause extensive cell membrane damage in primary human coronary artery endothelial cells and alter their cellular functions (Cronqvist, Salje et al. 2014). As the effects seen on HUVEC induced by miR-141-transfected HTR8/SVneo cells were stronger than those by miR-141-transfected JEG-3 cells, HTR8/SVneo cells were chosen for the further evaluation of EVs effects on tube formations.

HUVEC were seeded and cultured until tube formation (4 h), and subsequently, co-cultured with non-modified HTR8/SVneo cells. The characterized EVs were added to the 3D model and after 24 h, tube formations were evaluated through microscopy and image analysis. Treatment of non-transfected cells with EVs containing elevated miR-141 levels reduced the mean number of nodes at a similar intensity as transfection of HTR8/SVneo cells with overexpression of miR-141. But, effects of miR-141-containing EXOs were significantly ($p < 0.05$) higher compared with the effects of miR-141-containing MVs.

5.4. miR-141 and Preeclampsia: Results Overview

miRNAs have an involvement in many cellular processes, including angiogenesis. Their role on endothelial cells has been assessed by silencing Dicer (an endonuclease that cleaves the pre-miRNA into miRNA), using short interfering RNA in HUVEC causing an impairment on the development of the tube formations (Suarez and Sessa 2009).

The results showed that the overexpression of miR-141 in HTR8/SVneo cells diminished the ability to interact with HUVEC, inducing failure of maintenance of tube formations and causing an apparent reduction in the trophoblast invasion. This result can be related to some effects seen in preeclampsia, such as the inadequate remodeling of the uterine spiral arteries.

It can be compared that the results obtained in this work were similar to those shown in the patent US 20110059904 A1: *Serum-based, diagnostic, biological assay to predict pregnancy disorders.* This invention provides an assay that estimates if a woman is at risk of developing a disorder of pregnancy associated with trophoblast invasion (Sharma and Kalkunte 2011). It showed that serum from preeclamptic women, either mild or severe, disrupted the characteristic tube formations of the cells in co-culture, trophoblasts and endothelial cells (Kalkunte, Boij et al. 2010). As shown in Figure 21, the results obtained from the overexpression of miR-141 in HTR8/SVneo cells decreased the mean number of nodes between tubes, finding out the characteristic tube disruption as seen in experiments from Kalkunte et al., when using serum from severe preeclampsia.
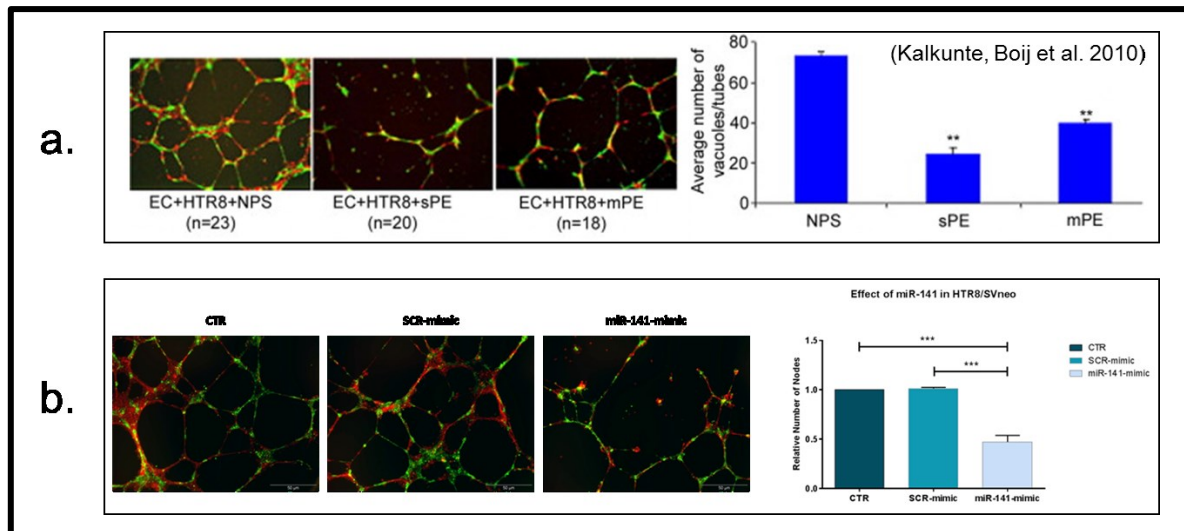
Figure 21. Comparison between the patent US 20110059904 A1 and results obtained with miR-141 overexpression. a) Preeclampsia serum, from both mild and severe conditions, disrupted the endothelial-trophoblast interaction (Taken from (Kalkunte, Boij et al. 2010). b) A highly significant reduction (*** $p < 0.001$) of the number of nodes was seen upon overexpression of miR-141 in HTR8/SVneo cells (Details on Figure 15).

Incorporation of miR-141-containing EVs on non-transfected HTR8/SVneo cells can also result in tube disruption, displaying the cell-cell communication through particles to nearby cells. Altogether, presented results indicate that miR-141 plays a role in the pathogenesis of preeclampsia.

Future experiments will be necessary to further clarify the specific involvement of miR-141 in preeclampsia. Those analyses should include the isolation and quantification of EVs from human preeclamptic serum, especially in regard to their miR-141 concentration, and their effects on the trophoblastic-endothelial interaction through the tube formation model. In this way, it could be proved that this miRNA is highly responsible for the effects seen in the impaired trophoblast invasion seen in the process of preeclampsia.

CONCLUSIONS

Preeclampsia is a hypertensive disorder that complicates between 2 - 8% of all pregnancies, probably related to improper EVT invasion into uterine spiral arteries and further deficient remodeling. During this process, trophoblast cells secrete miRNAs within EVs. Their amount and content differ between normal and pathological pregnancies, including preeclampsia. miR-141 expression is higher in placentas from preeclamptic compared to normal pregnancies. However, the function of miRNA-containing EVs on the intercellular communication between trophoblast and endothelial cells remains unclear.

In this study, it was explored the function of miR-141 in trophoblast-derived EVs on a 3D model for angiogenesis which allows the quantification of trophoblast-endothelial cell interaction through a specially adapted software. Levels of miR-141 expression were modified through transient transfection of trophoblastic cells to mimic levels as observed in preeclampsia. Analysis of HUVEC tube formation alterations was used for comparison between miR-141 overexpressing or inhibited HTR8/SVneo and JEG-3 cells, and the effects of their respective EVs.

Overexpression of miR-141 in HTR8/SVneo cells induced altered tube formations, an effect not perceived with modified JEG-3 cells. miR-141 containing EVs can be uptaken by non-transfected cells resulting also in tube disruption. Altogether, miR-141 may be involved in the regulation of the angiogenic potential of trophoblastic cells and their communication with endothelial cells through EVs, which may be associated with the pathogenesis of preeclampsia.

miR-141 in maternal plasma is detectable from early pregnancy onward and may be useful as a potential future diagnostic tool for pregnancy disorders. But further verification on clinical samples is needed to be studied before proper application as a molecular biomarker.

REFERENCES

- (2011). <u>WHO Recommendations for Prevention and Treatment of Pre-Eclampsia and Eclampsia</u>. Geneva.

- Abels, E. R. and X. O. Breakefield (2016). "Introduction to Extracellular Vesicles: Biogenesis, RNA Cargo Selection, Content, Release, and Uptake." <u>Cell Mol Neurobiol</u> **36**(3): 301-312.

- Ahmed, A. and W. Ramma (2015). "Unravelling the theories of pre-eclampsia: are the protective pathways the new paradigm?" <u>Br J Pharmacol</u> **172**(6): 1574-1586.

- Aldo, P. B., G. Krikun, I. Visintin, C. Lockwood, R. Romero and G. Mor (2007). "A novel three-dimensional in vitro system to study trophoblast-endothelium cell interactions." <u>Am J Reprod Immunol</u> **58**(2): 98-110.

- Alvarez, A. M., M. J. Mulla, L. W. Chamley, A. P. Cadavid and V. M. Abrahams (2015). "Aspirin-triggered lipoxin prevents antiphospholipid antibody effects on human trophoblast migration and endothelial cell interactions." <u>Arthritis Rheumatol</u> **67**(2): 488-497.

- Bilban, M., S. Tauber, P. Haslinger, J. Pollheimer, L. Saleh, H. Pehamberger, O. Wagner and M. Knofler (2010). "Trophoblast invasion: assessment of cellular models using gene expression signatures." <u>Placenta</u> **31**(11): 989-996.

- Bokslag, A., M. van Weissenbruch, B. W. Mol and C. J. de Groot (2016). "Preeclampsia; short and long-term consequences for mother and neonate." <u>Early Hum Dev</u>.

- Bulmer, J. N., G. J. Burton, S. Collins, T. Cotechini, I. P. Crocker, B. A. Croy, S. Cvitic, M. Desforges, R. Deshpande, M. Gasperowicz, T. Groten, G. Haugen, U. Hiden, A. J. Host, M. Jirkovska, T. Kiserud, J. Konig, L. Leach, P. Murthi, R. Pijnenborg, O. N. Sadekova, C. M. Salafia, N. Schlabritz-Loutsevitch, J. Stanek, A. E. Wallace, F. Westermeier, J. Zhang and G. E. Lash (2012). "IFPA Meeting 2011 workshop report II: Angiogenic signaling and regulation of fetal endothelial function; placental and fetal circulation and growth; spiral artery remodeling." <u>Placenta</u> **33 Suppl**: S9-S14.

- Burton, G. J. and E. Jauniaux (2015). "What is the placenta?" <u>Am J Obstet Gynecol</u> **213**(4 Suppl): S6 e1, S6-8.

- Burton, G. J., A. W. Woods, E. Jauniaux and J. C. Kingdom (2009). "Rheological and physiological consequences of conversion of the maternal spiral arteries for uteroplacental blood flow during human pregnancy." Placenta **30**(6): 473-482.

- Chim, S. S., T. K. Shing, E. C. Hung, T. Y. Leung, T. K. Lau, R. W. Chiu and Y. M. Lo (2008). "Detection and characterization of placental microRNAs in maternal plasma." Clin Chem **54**(3): 482-490.

- Colombo, M., G. Raposo and C. Thery (2014). "Biogenesis, secretion, and intercellular interactions of exosomes and other extracellular vesicles." Annu Rev Cell Dev Biol **30**: 255-289.

- Craici, I. M., S. J. Wagner, T. L. Weissgerber, J. P. Grande and V. D. Garovic (2014). "Advances in the pathophysiology of pre-eclampsia and related podocyte injury." Kidney Int **86**(2): 275-285.

- Cretoiu, D., J. Xu, J. Xiao, N. Suciu and S. M. Cretoiu (2016). "Circulating MicroRNAs as Potential Molecular Biomarkers in Pathophysiological Evolution of Pregnancy." Dis Markers **2016**: 3851054.

- Cronqvist, T., K. Salje, M. Familari, S. Guller, H. Schneider, C. Gardiner, I. L. Sargent, C. W. Redman, M. Morgelin, B. Akerstrom, M. Gram and S. R. Hansson (2014). "Syncytiotrophoblast vesicles show altered micro-RNA and haemoglobin content after ex-vivo perfusion of placentas with haemoglobin to mimic preeclampsia." PLoS One **9**(2): e90020.

- Cunningham, F. G. and J. W. Williams (2010). Williams obstetrics. New York, McGraw-Hill Medical.

- DeCicco-Skinner, K. L., G. H. Henry, C. Cataisson, T. Tabib, J. C. Gwilliam, N. J. Watson, E. M. Bullwinkle, L. Falkenburg, R. C. O'Neill, A. Morin and J. S. Wiest (2014). "Endothelial cell tube formation assay for the in vitro study of angiogenesis." J Vis Exp(91): e51312.

- Degner, K., R. R. Magness and D. M. Shah (2017). "Establishment of the Human Uteroplacental Circulation: A Historical Perspective." Reprod Sci **24**(5): 753-761.

- Escudero, C. A., K. Herlitz, F. Troncoso, J. Acurio, C. Aguayo, J. M. Roberts, G. Truong, G. Duncombe, G. Rice and C. Salomon (2016). "Role of Extracellular Vesicles and microRNAs on Dysfunctional Angiogenesis during Preeclamptic Pregnancies." Front Physiol **7**: 98.

- Filipe, V., A. Hawe and W. Jiskoot (2010). "Critical evaluation of Nanoparticle Tracking Analysis (NTA) by NanoSight for the measurement of nanoparticles and protein aggregates." Pharm Res **27**(5): 796-810.

- Gao, Y., B. Feng, S. Han, K. Zhang, J. Chen, C. Li, R. Wang and L. Chen (2016). "The Roles of MicroRNA-141 in Human Cancers: From Diagnosis to Treatment." Cell Physiol Biochem **38**(2): 427-448.

- Gardiner, C., Y. J. Ferreira, R. A. Dragovic, C. W. Redman and I. L. Sargent (2013). "Extracellular vesicle sizing and enumeration by nanoparticle tracking analysis." J Extracell Vesicles **2**.

- Gilani, S. I., T. L. Weissgerber, V. D. Garovic and M. Jayachandran (2016). "Preeclampsia and Extracellular Vesicles." Curr Hypertens Rep **18**(9): 68.

- Gongora, M. C. and N. K. Wenger (2015). "Cardiovascular Complications of Pregnancy." Int J Mol Sci **16**(10): 23905-23928.

- Graham, C. H., T. S. Hawley, R. G. Hawley, J. R. MacDougall, R. S. Kerbel, N. Khoo and P. K. Lala (1993). "Establishment and characterization of first trimester human trophoblast cells with extended lifespan." Exp Cell Res **206**(2): 204-211.

- Gregory, R. I. and R. Shiekhattar (2005). "MicroRNA biogenesis and cancer." Cancer Res **65**(9): 3509-3512.

- Ha, M. and V. N. Kim (2014). "Regulation of microRNA biogenesis." Nat Rev Mol Cell Biol **15**(8): 509-524.

- Highet, A. R., V. J. Zhang, G. K. Heinemann and C. T. Roberts (2012). "Use of Matrigel in culture affects cell phenotype and gene expression in the first trimester trophoblast cell line HTR8/SVneo." Placenta **33**(7): 586-588.

- Humphries, B. and C. Yang (2015). "The microRNA-200 family: small molecules with novel roles in cancer development, progression and therapy." Oncotarget **6**(9): 6472-6498.

- Huppertz, B. (2008). "Placental origins of preeclampsia: challenging the current hypothesis." Hypertension **51**(4): 970-975.

- Imakawa, K., R. Bai, H. Fujiwara, A. Ideta, Y. Aoyagi and K. Kusama (2017). "Continuous model of conceptus implantation to the maternal endometrium." J Endocrinol **233**(1): R53-R65.

- Johnstone, R. M., M. Adam, J. R. Hammond, L. Orr and C. Turbide (1987). "Vesicle formation during reticulocyte maturation. Association of plasma

membrane activities with released vesicles (exosomes)." J Biol Chem **262**(19): 9412-9420.

- Kalkunte, S., R. Boij, W. Norris, J. Friedman, Z. Lai, J. Kurtis, K. H. Lim, J. F. Padbury, L. Matthiesen and S. Sharma (2010). "Sera from preeclampsia patients elicit symptoms of human disease in mice and provide a basis for an in vitro predictive assay." Am J Pathol **177**(5): 2387-2398.

- Kalkunte, S., Z. Lai, W. E. Norris, L. A. Pietras, N. Tewari, R. Boij, S. Neubeck, U. R. Markert and S. Sharma (2009). "Novel approaches for mechanistic understanding and predicting preeclampsia." J Reprod Immunol **83**(1-2): 134-138.

- Kleinman, H. K., M. L. McGarvey, L. A. Liotta, P. G. Robey, K. Tryggvason and G. R. Martin (1982). "Isolation and characterization of type IV procollagen, laminin, and heparan sulfate proteoglycan from the EHS sarcoma." Biochemistry **21**(24): 6188-6193.

- Kohler, P. O. and W. E. Bridson (1971). "Isolation of hormone-producing clonal lines of human choriocarcinoma." J Clin Endocrinol Metab **32**(5): 683-687.

- Li, H., Q. Ge, L. Guo and Z. Lu (2013). "Maternal plasma miRNAs expression in preeclamptic pregnancies." Biomed Res Int **2013**: 970265.

- Malloy, A. (2011). "Count, size and visualize nanoparticles." Materials Today **14**(4): 170-173.

- Marquez-Curtis, L. A., A. B. Sultani, L. E. McGann and J. A. Elliott (2016). "Beyond membrane integrity: Assessing the functionality of human umbilical vein endothelial cells after cryopreservation." Cryobiology **72**(3): 183-190.

- Mol, B. W., C. T. Roberts, S. Thangaratinam, L. A. Magee, C. J. de Groot and G. J. Hofmeyr (2016). "Pre-eclampsia." Lancet **387**(10022): 999-1011.

- Morales-Prieto, D. M., W. Chaiwangyen, S. Ospina-Prieto, U. Schneider, J. Herrmann, B. Gruhn and U. R. Markert (2012). "MicroRNA expression profiles of trophoblastic cells." Placenta **33**(9): 725-734.

- Morales-Prieto, D. M., E. Schleussner and U. R. Markert (2011). "Reduction in miR-141 is induced by leukemia inhibitory factor and inhibits proliferation in choriocarcinoma cell line JEG-3." Am J Reprod Immunol **66 Suppl 1**: 57-62.

- O'Tierney-Ginn, P. F. and G. E. Lash (2014). "Beyond pregnancy: modulation of trophoblast invasion and its consequences for fetal growth and long-term children's health." J Reprod Immunol **104-105**: 37-42.

- Ospina-Prieto, S., W. Chaiwangyen, J. Herrmann, T. Groten, E. Schleussner, U. R. Markert and D. M. Morales-Prieto (2016). "MicroRNA-141 is upregulated in preeclamptic placentae and regulates trophoblast invasion and intercellular communication." Transl Res **172**: 61-72.

- Ouyang, Y., J. F. Mouillet, C. B. Coyne and Y. Sadovsky (2014). "Review: placenta-specific microRNAs in exosomes - good things come in nano-packages." Placenta **35 Suppl**: S69-73.

- Pecot, C. V., R. Rupaimoole, D. Yang, R. Akbani, C. Ivan, C. Lu, S. Wu, H. D. Han, M. Y. Shah, C. Rodriguez-Aguayo, J. Bottsford-Miller, Y. Liu, S. B. Kim, A. Unruh, V. Gonzalez-Villasana, L. Huang, B. Zand, M. Moreno-Smith, L. S. Mangala, M. Taylor, H. J. Dalton, V. Sehgal, Y. Wen, Y. Kang, K. A. Baggerly, J. S. Lee, P. T. Ram, M. K. Ravoori, V. Kundra, X. Zhang, R. Ali-Fehmi, A. M. Gonzalez-Angulo, P. P. Massion, G. A. Calin, G. Lopez-Berestein, W. Zhang and A. K. Sood (2013). "Tumour angiogenesis regulation by the miR-200 family." Nat Commun **4**: 2427.

- Powe, C. E., R. J. Levine and S. A. Karumanchi (2011). "Preeclampsia, a disease of the maternal endothelium: the role of antiangiogenic factors and implications for later cardiovascular disease." Circulation **123**(24): 2856-2869.

- Raposo, G. and W. Stoorvogel (2013). "Extracellular vesicles: exosomes, microvesicles, and friends." J Cell Biol **200**(4): 373-383.

- Ratajczak, J., K. Miekus, M. Kucia, J. Zhang, R. Reca, P. Dvorak and M. Z. Ratajczak (2006). "Embryonic stem cell-derived microvesicles reprogram hematopoietic progenitors: evidence for horizontal transfer of mRNA and protein delivery." Leukemia **20**(5): 847-856.

- Salomon, C., S. Yee, K. Scholz-Romero, M. Kobayashi, K. Vaswani, D. Kvaskoff, S. E. Illanes, M. D. Mitchell and G. E. Rice (2014). "Extravillous trophoblast cells-derived exosomes promote vascular smooth muscle cell migration." Front Pharmacol **5**: 175.

- Senfter, D., S. Madlener, G. Krupitza and R. M. Mader (2016). "The microRNA-200 family: still much to discover." Biomol Concepts **7**(5-6): 311-319.

- Sharma, S. and S. Kalkunte (2011). Serum-based, diagnostic, biological assay to predict pregnancy disorders, Google Patents.

- Soares, M. J., D. Chakraborty, K. Kubota, S. J. Renaud and M. A. Rumi (2014). "Adaptive mechanisms controlling uterine spiral artery remodeling during the establishment of pregnancy." Int J Dev Biol **58**(2-4): 247-259.

- Sokolov, D. I., T. Y. Lvova, L. S. Okorokova, K. L. Belyakova, A. R. Sheveleva, O. I. Stepanova, V. A. Mikhailova and S. A. Sel'kov (2017). "Effect of Cytokines on the Formation Tube-Like Structures by Endothelial Cells in the Presence of Trophoblast Cells." Bull Exp Biol Med **163**(1): 148-158.

- Steegers, E. A., P. von Dadelszen, J. J. Duvekot and R. Pijnenborg (2010). "Pre-eclampsia." Lancet **376**(9741): 631-644.

- Strimbu, K. and J. A. Tavel (2010). "What are biomarkers?" Curr Opin HIV AIDS **5**(6): 463-466.

- Su, R. W. and A. T. Fazleabas (2015). "Implantation and Establishment of Pregnancy in Human and Nonhuman Primates." Adv Anat Embryol Cell Biol **216**: 189-213.

- Suarez, Y. and W. C. Sessa (2009). "MicroRNAs as novel regulators of angiogenesis." Circ Res **104**(4): 442-454.

- Suman, P. and S. K. Gupta (2012). "Comparative analysis of the invasion-associated genes expression pattern in first trimester trophoblastic (HTR-8/SVneo) and JEG-3 choriocarcinoma cells." Placenta **33**(10): 874-877.

- Szatanek, R., M. Baj-Krzyworzeka, J. Zimoch, M. Lekka, M. Siedlar and J. Baran (2017). "The Methods of Choice for Extracellular Vesicles (EVs) Characterization." Int J Mol Sci **18**(6).

- Tannetta, D., I. Masliukaite, M. Vatish, C. Redman and I. Sargent (2016). "Update of syncytiotrophoblast derived extracellular vesicles in normal pregnancy and preeclampsia." J Reprod Immunol.

- Thery, C. (2011). "Exosomes: secreted vesicles and intercellular communications." F1000 Biol Rep **3**: 15.

- Thery, C., S. Amigorena, G. Raposo and A. Clayton (2006). "Isolation and characterization of exosomes from cell culture supernatants and biological fluids." Curr Protoc Cell Biol **Chapter 3**: Unit 3 22.

- Townsend, R., P. O'Brien and A. Khalil (2016). "Current best practice in the management of hypertensive disorders in pregnancy." Integr Blood Press Control **9**: 79-94.

- Tranquilli, A. L., G. Dekker, L. Magee, J. Roberts, B. M. Sibai, W. Steyn, G. G. Zeeman and M. A. Brown (2014). "The classification, diagnosis and management of the hypertensive disorders of pregnancy: A revised statement from the ISSHP." Pregnancy Hypertens **4**(2): 97-104.

- Uzan, J., M. Carbonnel, O. Piconne, R. Asmar and J. M. Ayoubi (2011). "Pre-eclampsia: pathophysiology, diagnosis, and management." Vasc Health Risk Manag **7**: 467-474.

- Wang, Y. and S. Zhao (2010). Vascular Biology of the Placenta. San Rafael (CA).

- Whitley, G. S. and J. E. Cartwright (2010). "Cellular and molecular regulation of spiral artery remodelling: lessons from the cardiovascular field." Placenta **31**(6): 465-474.

- Wolf, P. (1967). "The nature and significance of platelet products in human plasma." Br J Haematol **13**(3): 269-288.

APPENDIX

LISTS OF TABLES AND FIGURES

o Figure 21. Comparison between the patent US 20160033484 A1 and results obtained with miR-141 overexpression.

- Tables
  o Table 1. Frequent cargo of EVs, sub-classified in proteins, lipids, and nucleic acids.
  o Table 2. Classification of EVs based on their biogenesis
  o Table 3. Comparison of the mean size of EXO- and MV-enriched fractions produced by HTR8/SVneo cells as assessed by NTA.
  o Table 4. Mean concentration of EVs obtained from HTR8/SVneo cells transfected with miR-141-mimic.

ACKNOWLEDGEMENT

To my parents, with whom I will be forever grateful. Thanks for everything, for the support, concern, love and motivational messages. To my siblings, thanks for those (de)stressed moments shared traveling together.

To Prof. Dr. Udo Markert, thanks for allowing me to accomplish my studies in this laboratory and for all the support and help during this time. To all the Placenta-Lab team, especially Drs. Diana-María Morales-Prieto and Rodolfo Favaro, for the advice, supervision, support and the time spent. Thanks also to Dr. Wittaya Chaiwangyen for the good vibes 555.

To Silke and Prof. Dr. Bernd Luckas, whom I appreciate as part of my family; thanks for the advice and morning conversations. For many other things, I will be always grateful.

To whom I estimate and appreciate, thanks Erik W. for your motivation, encouragement, and your smile. To my friends in Panama, despite the distance and time differences, thanks to them all, especially Laura and Wister. Thank you for listening, reading my messages, and always making every moment a funny and interesting story.

To the German Academic Exchange Service (DAAD) for the economic support these years and the opportunity to live and study abroad.

Ehrenwörtliche Erklärung

Hiermit erkläre ich, dass mir die Promotionsordnung der Medizinischen Fakultät der Friedrich-Schiller-Universität bekannt ist,

ich die Dissertation selbst angefertigt habe und alle von mir benutzten Hilfsmittel, persönlichen Mitteilungen und Quellen in meiner Arbeit angegeben sind,

mich folgende Personen bei der Auswahl und Auswertung des Materials sowie bei der Herstellung des Manuskripts unterstützt haben: Prof. Dr. Udo Markert und Dr. Diana Morales-Prieto,

die Hilfe eines Promotionsberaters nicht in Anspruch genommen wurde und dass Dritte weder unmittelbar noch mittelbar geldwerte Leistungen von mir für Arbeiten erhalten haben, die im Zusammenhang mit dem Inhalt der vorgelegten Dissertation stehen,

dass ich die Dissertation noch nicht als Prüfungsarbeit für eine staatliche oder andere wissenschaftliche Prüfung eingereicht habe und

dass ich die gleiche, eine in wesentlichen Teilen ähnliche oder eine andere Abhandlung nicht bei einer anderen Hochschule als Dissertation eingereicht habe.

Jena, 20.11. 2017   Unterschrift des Verfassers